

The EDM inverse problem: Identifying the sources of CP violation and PQ breaking with electric dipole moments

Kiwoon Choi¹ and Sang Hui Im²

*Particle Theory and Cosmology Group, Center for Theoretical Physics of the Universe,
Institute for Basic Science (IBS), Daejeon 34126, Korea*

ABSTRACT: Many extensions of the Standard Model (SM) generically introduce new sources of CP violation, which can induce observable P -odd and T -odd permanent electric dipole moments (EDMs) of nuclei, atoms, and molecules. A future observation of nonvanishing EDMs would therefore provide a sensitive probe of physics beyond the SM, while also posing a nontrivial inverse problem: identifying their underlying ultraviolet origin. In this work, we identify six representative classes of CP-violating effective operators near the QCD scale, including the QCD θ -term, that are particularly relevant for low-energy EDMs and can arise in a broad range of SM extensions. We show that these operator classes lead to distinct EDM patterns across different systems, thereby enabling discrimination among them through experimentally measured EDMs. We further emphasize that EDM measurements can shed light on the origin of the vacuum expectation value of the QCD axion. In particular, they may help distinguish whether a nonzero axion vacuum expectation value is predominantly induced by high-scale Peccei–Quinn symmetry-breaking effects, such as those associated with quantum gravity, or by the interplay between beyond-the-SM CP violation and the QCD anomaly.

¹email: kchoi@ibs.re.kr

²email: imsanghui@ibs.re.kr

Contents

1	Introduction	1
2	UV sources for CP violation and PQ breaking	3
2.1	QCD axion effect	5
2.2	Renormalization effect	7
3	CP-odd interactions at IR	8
3.1	Nucleon electric dipole moments	8
3.2	CP-odd pion-nucleon interactions	12
3.3	CP-odd four-nucleon contact interactions	15
3.4	Semi-leptonic interactions	16
4	Electric dipole moments of nuclei, atoms, and molecules	17
4.1	Light nuclei and diamagnetic atoms	18
4.2	Paramagnetic systems	19
5	Identification of the UV sources with EDM data	21
5.1	Hadronic sources	21
5.1.1	Single source	21
5.1.2	Multiple sources	23
5.2	(Semi-)leptonic sources	27
6	Conclusions	28
A	Naïve Dimensional Analysis for hadronic CP-odd quantities	29

1 Introduction

Despite its tremendous success, the Standard Model (SM) of particle physics requires extension, as it does not contain a viable dark matter candidate and cannot account for baryogenesis (see, e.g., [1] for a review) or neutrino masses. Physics beyond the Standard Model (BSM) that addresses these problems generically introduces new sources of CP violation. Such CP violation can be transmitted to the SM sector, giving rise to sizable P -odd and T -odd permanent electric dipole moments (EDMs) of nuclei, atoms, and molecules [2–4]. Roughly speaking, BSM physics at energy scales ranging from the TeV to the PeV scale can induce EDMs that may be observable in near-future experiments [5].

Once nonvanishing EDMs are observed, a central question will be the identification of the underlying ultraviolet (UV) physics responsible for the observed signals. In principle, properties of the underlying UV physics may be inferred, at least partially, from the

available EDM data. We refer to the problem of identifying the specific underlying physics responsible for a given set of EDM measurements as *the EDM inverse problem*. This problem has been investigated in a number of earlier works, both in terms of CP-violating (CPV) operators at the hadronic scale [2, 6–8] and at higher energy scales [9–13].

In this work, we revisit the EDM inverse problem. We first identify six important classes of CPV operators around the QCD scale (~ 1 GeV) that are particularly relevant for low-energy EDMs and can arise from broad classes of well-motivated BSM scenarios. These include the QCD θ -term, which already exists in the SM; three additional classes of hadronic operators associated with the EDMs and chromo-EDMs of light quarks and gluons; and two classes of (semi-)leptonic operators, including the electron EDM. We then demonstrate that the ratios of EDMs of nuclei, atoms, and molecules predicted by these operator classes exhibit distinctive patterns, depending on which class of CPV operators dominates. Our approach is similar in spirit to previous studies [9–13], but we present updated and more quantitative results by incorporating state-of-the-art theoretical inputs for atomic and molecular EDMs, as well as hadronic observables induced by CPV operators at the QCD scale.

An intriguing aspect of EDM physics is its connection to the Peccei–Quinn (PQ) mechanism, which addresses the strong CP problem via the QCD axion [14–16]. As discussed in Refs. [11–13], patterns of nuclear and atomic EDMs can provide valuable information about the underlying mechanism responsible for resolving the strong CP problem. Hadronic BSM CPV operators generically induce large quantum corrections to the QCD θ parameter [11, 12, 17, 18], thereby spoiling ultraviolet solutions to the strong CP problem, such as the Nelson–Barr mechanism [19, 20]. Therefore, if experimentally observed EDM ratios are consistent with predictions from hadronic BSM CPV operators while being inconsistent with those from the QCD θ -dominated scenario, this would point toward the necessity of an infrared solution to the strong CP problem, such as the PQ mechanism, to explain the smallness of θ [11].

In our previous work [13], we generalized and reinterpreted this observation by allowing for the possibility of a simply fine-tuned θ , and showed that certain classes of hadronic CPV operators, with or without the PQ mechanism, can be distinguished by their characteristic EDM ratios. In particular, we argued that EDM measurements may reveal whether a nonzero vacuum expectation value (VEV) of the QCD axion predominantly originates from PQ-symmetry breaking at high scales, such as quantum-gravitational effects, or from the interplay between hadronic BSM CPV operators and the QCD anomaly. In other words, EDM data may provide insight into the dominant PQ-breaking source beyond the QCD anomaly, which is crucial for understanding the axion quality problem (see, e.g., [21] for a recent review). In the present work, we extend this analysis by including (i) all potentially important BSM CPV operators arising from well-motivated scenarios, (ii) EDMs of light nuclei and diamagnetic atoms targeted by ongoing and planned experiments, and (iii) scenarios in which multiple classes of CPV operators contribute comparably to the observed EDMs.

We find that EDM measurements of light nuclei, such as the neutron, proton, deuteron, and helion, are particularly powerful for discriminating among the four classes of hadronic

operators, including the θ -term and the EDMs and chromo-EDMs of quarks and gluons. This observation strongly motivates storage-ring experiments that can directly measure the EDMs of charged light nuclei [22]. In contrast, EDM data from diamagnetic atoms with heavy nuclei, such as ^{199}Hg , ^{129}Xe , and ^{171}Yb , may provide suggestive information about the UV source but are unlikely to be conclusive due to large theoretical uncertainties. Octupole-deformed systems, such as ^{225}Ra , may offer improved sensitivity in this respect, although still less than that of light nuclei. We also discuss how EDM measurements of two different paramagnetic molecules, such as HfF^+ and ThO , can disentangle the electron EDM from the electron–nucleon CPV coupling as previously analyzed in [23], and we further explore the implications for hadronic CPV sources.

It should be emphasized that many of the matching relations used to connect CPV operators at the QCD scale to experimentally measured EDMs are subject to intrinsic uncertainties that cannot be reliably quantified with the current level of theoretical understanding of the relevant QCD, nuclear and atomic physics effects. Our results should therefore be interpreted with these uncertainties in mind. Our primary goal is to assess how far one can proceed using the currently available theoretical inputs, while also motivating future theoretical efforts toward a more quantitative understanding of the matching relations relevant for EDMs.

This paper is organized as follows. In Sec. 2, we identify six classes of CPV operators around the QCD scale that are particularly relevant for low-energy EDMs and arise from broad classes of well-motivated BSM scenarios. We also discuss the radiative corrections to these operators from the BSM scale down to the QCD scale, as well as the impact of certain hadronic operators on the PQ mechanism that solves the strong CP problem via a QCD axion field whose vacuum expectation value can be identified with the QCD θ parameter. In Sec. 3, we describe the leading infrared CPV operators at the hadronic level below the QCD scale and present updated results for their matching to the CPV sources at the QCD scale. In Sec. 4, we summarize state-of-the-art calculations of EDMs for light nuclei, atoms, and molecules, together with experimental prospects. Section 5 contains the main results of this work, where we demonstrate that the six classes of CPV operators at the QCD scale, either with or without the PQ mechanism, can be distinguished using appropriate combinations of EDM data. We conclude in Sec. 6.

2 UV sources for CP violation and PQ breaking

Permanent electric dipole moments (EDMs) of elementary particles and nucleons arise from CP-violating (CPV) interactions among Standard Model (SM) particles. In general, gauge-invariant CPV interactions of SM fields above the electroweak scale can be written as

$$\mathcal{L}_{\text{CPV}}(\mu > m_W) = \mathcal{L}_{\text{KM}} + \frac{g_s^2}{32\pi^2} \bar{\theta} G_{\mu\nu}^a \tilde{G}^{a\mu\nu} + \mathcal{L}_6 + \dots, \quad (2.1)$$

where \mathcal{L}_{KM} denotes the charged-current weak interactions containing the Kobayashi–Maskawa (KM) phase, $\bar{\theta}$ is the QCD vacuum angle defined in the basis where the quark mass matrices

are real and diagonal, and \mathcal{L}_6 represents a set of CPV dimension-six operators constructed from SM fields. The ellipsis includes the dimension-five Weinberg operator responsible for Majorana neutrino masses, as well as operators of dimension greater than six. We neglect these contributions, as they are suppressed either by small neutrino masses or by additional powers of the heavy mass scale. We also neglect the contribution of \mathcal{L}_{KM} to EDMs, since it is highly suppressed. This suppression arises because EDMs are flavor-diagonal observables, whereas CP violation in \mathcal{L}_{KM} is encoded in flavor-changing interactions (see, e.g., [5]).

A complete classification of operators in \mathcal{L}_6 is given in Ref. [24]. However, at the QCD scale $\mu \sim 1$ GeV, many of these operators are integrated out, leaving the following operators that provide the leading contributions to EDMs:

$$\mathcal{L}_\theta = \frac{g_s^2}{32\pi^2} \bar{\theta} G_{\mu\nu}^a \tilde{G}^{a\mu\nu}, \quad (2.2)$$

$$\mathcal{L}_{\text{dipole}} = \frac{1}{3} w f^{abc} G_\alpha^{a\mu} G_\mu^{b\delta} \tilde{G}_\delta^{c\alpha} - \frac{i}{2} \sum_{q=u,d,s} \tilde{d}_q g_s \bar{q} \sigma^{\mu\nu} G_{\mu\nu} \gamma_5 q - \frac{i}{2} \sum_{f=u,d,s,e} d_f \bar{f} \sigma^{\mu\nu} F_{\mu\nu} \gamma_5 f, \quad (2.3)$$

$$\mathcal{L}_{4\text{-fermi}} = \left(i \sum_{D=d,s,b} \text{Im}(C_{eeDD}) (e_L^\dagger e_R) (\bar{D}_R D_L) + \text{h.c.} \right) + \dots, \quad (2.4)$$

where $\mathcal{L}_{\text{dipole}}$ includes the Weinberg three-gluon operator, which can be interpreted as a gluonic chromo-electric dipole moment (CEDM), the light-quark CEDMs, and the EDMs of light quarks and the electron. The ellipsis in $\mathcal{L}_{4\text{-fermi}}$ denotes CPV four-quark operators and additional (semi-)leptonic operators that are not considered in this work.

The SM and various beyond-the-SM (BSM) scenarios can be characterized by a small number of dominant operators among those appearing in Eqs. (2.2)–(2.4). In the SM, the QCD θ -term \mathcal{L}_θ provides the dominant source of EDMs, if nonzero EDMs are observed in the near future, since contributions from the KM phase are far below current experimental sensitivities. In contrast, one or more dipole operators in $\mathcal{L}_{\text{dipole}}$ can dominate in well-motivated BSM scenarios, such as supersymmetric extensions of the SM [25–27], two-Higgs-doublet models (2HDMs) [28], and universal theories [29, 30], in which the BSM sector communicates with the SM primarily through gauge interactions or the Higgs portal.

The semi-leptonic four-fermion operators in $\mathcal{L}_{4\text{-fermi}}$ can be particularly important in the minimal supersymmetric Standard Model (MSSM) or the type-II 2HDM in the large $\tan\beta$ regime, where their effects are enhanced by the large value of $\tan\beta$ [31]. By contrast, other types of CPV four-fermion operators, including four-quark operators, are typically suppressed by the small SM Yukawa couplings of light fermions in such BSM scenarios [28, 32, 33]. Certain four-quark operators can play an important role in left–right symmetric models [10, 12], which we do not consider here.

We therefore focus on six potentially important classes of UV CPV parameters arising from the SM and various BSM scenarios:

$$X_i^{\text{UV}} \in \left\{ \bar{\theta}, w, \tilde{d}_q, d_q, d_e, \text{Im}(C_{eeDD}) \right\}, \quad (2.5)$$

where $q = u, d, s$ and $D = d, s, b$. Parameters within the same class typically give comparable contributions to EDMs, while those from different classes can differ by orders of magnitude.

In many BSM scenarios, chirality violation in quark (C)EDMs originates from quark masses, implying a relation between strange- and down-quark (C)EDMs,

$$\tilde{d}_s = \frac{m_s}{m_d} \tilde{d}_d, \quad d_s = \frac{m_s}{m_d} d_d. \quad (2.6)$$

By contrast, the up-quark (C)EDM is not generally related to the down-quark (C)EDM by a simple mass ratio, due to differences in electric charges and the $\tan\beta$ dependence of Yukawa couplings for up- and down-type quarks. Accordingly, we will often impose Eq. (2.6) while treating d_u (\tilde{d}_u) and d_d (\tilde{d}_d) as independent parameters.

The different classes of CPV parameters in Eq. (2.5) are related to each other in some cases. Below, we discuss two important effects that lead to nontrivial relations among them.

2.1 QCD axion effect

If the Peccei–Quinn (PQ) mechanism is realized to solve the strong CP problem, the QCD θ term is replaced by the axion coupling to gluons,

$$\frac{g_s^2}{32\pi^2} \frac{a}{f_a} G_{\mu\nu}^a \tilde{G}^{a\mu\nu}, \quad (2.7)$$

where $a(x)$ denotes the axion field with decay constant f_a . This coupling arises from the breaking of the PQ symmetry $U(1)_{\text{PQ}}$ by the QCD anomaly and generates the standard QCD axion potential,

$$V_{\text{QCD}}(a) \sim m_\pi^2 f_\pi^2 \cos\left(\frac{a}{f_a}\right). \quad (2.8)$$

It also implies that the QCD θ parameter is determined by the vacuum expectation value (VEV) of the axion field as

$$\bar{\theta} = \frac{\langle a \rangle}{f_a}. \quad (2.9)$$

If the axion potential is entirely dominated by the QCD contribution V_{QCD} , minimizing the potential yields $\bar{\theta} = 0$, thereby solving the strong CP problem. On the other hand, in the presence of CP-odd effective interactions at the QCD scale,

$$\mathcal{L}_{\text{BSM}} = \sum_i \lambda_i \mathcal{O}_i, \quad (2.10)$$

which may arise from BSM physics at higher scales, the axion potential receives an additional contribution estimated as [13]

$$\delta V_{\text{BSM}}(a) \sim \sum_i \lambda_i \int d^4x \left\langle \frac{g_s^2}{32\pi^2} G \tilde{G}(x) \mathcal{O}_i(0) \right\rangle_{a=0} \frac{a}{f_a} + \mathcal{O}\left(\frac{a}{f_a}\right)^2. \quad (2.11)$$

This additional contribution shifts the axion VEV away from the CP-conserving point, leading to a nonzero effective QCD θ parameter,

$$\bar{\theta}_{\text{BSM}} = \frac{\langle a \rangle_{\text{BSM}}}{f_a} \sim \frac{\sum_i \lambda_i \int d^4x \left\langle \frac{g_s^2}{32\pi^2} G\tilde{G}(x) \mathcal{O}_i(0) \right\rangle_{a=0}}{f_\pi^2 m_\pi^2}. \quad (2.12)$$

To solve the strong CP problem, this induced θ parameter must satisfy the experimental bound $|\bar{\theta}_{\text{BSM}}| \lesssim 10^{-10}$, which imposes stringent constraints on the Wilson coefficients λ_i of the BSM-induced effective interactions in Eq. (2.10).

Among the operators listed in Eqs. (2.2)–(2.4), quark chromo-electric dipole moments (CEDMs) and the gluon CEDM (the Weinberg three-gluon operator) can generate sizable contributions to $\bar{\theta}_{\text{BSM}}$. The axion VEV induced by quark CEDMs has been computed using QCD sum rules in Ref. [34], whereas no dedicated calculation exists for the gluon CEDM contribution. Employing naïve dimensional analysis (NDA) for the latter, one finds

$$\bar{\theta}_{\text{BSM}} = \frac{\langle a \rangle_{\text{BSM}}}{f_a} = \frac{m_0^2}{2} \sum_{q=u,d,s} \frac{\tilde{d}_q}{m_q} + \mathcal{O}(4\pi f_\pi^2 w), \quad (2.13)$$

where $m_0^2 \equiv g_s \langle \bar{q} G^{\mu\nu} \sigma_{\mu\nu} q \rangle / \langle \bar{q} q \rangle = 0.8(1) \text{ GeV}^2$ [35].

Another important source of a nonzero axion VEV arises from PQ-symmetry breaking effects other than the QCD anomaly, such as those induced by quantum gravity. Since global symmetries are generally expected to be violated by quantum gravity, the PQ symmetry associated with the QCD axion is expected to be broken near the quantum gravity scale [36–42]. For example, string or brane instantons in string theory, as well as gravitational wormholes, can generate an axion potential of the form (see, e.g., [43, 44] for reviews)

$$\delta V_{\text{UV}} = \Lambda_{\text{UV}}^4 e^{-S_{\text{ins}}} \cos\left(\frac{a}{f_a} + \delta_{\text{UV}}\right), \quad (2.14)$$

where Λ_{UV} is a model-dependent UV scale, S_{ins} is the Euclidean instanton action, and δ_{UV} is a CP-violating phase generically of order unity. This potential induces an axion VEV

$$\bar{\theta}_{\text{UV}} = \frac{\langle a \rangle_{\text{UV}}}{f_a} \sim e^{-S_{\text{ins}}} \frac{\Lambda_{\text{UV}}^4 \sin \delta_{\text{UV}}}{f_\pi^2 m_\pi^2}, \quad (2.15)$$

which can naturally satisfy $|\bar{\theta}_{\text{UV}}| \lesssim 10^{-10}$ for moderately large values of S_{ins} .

In general, the total axion VEV receives contributions from both sources,

$$\bar{\theta}_{\text{PQ}} \equiv \frac{\langle a \rangle}{f_a} = \bar{\theta}_{\text{UV}} + \bar{\theta}_{\text{BSM}}. \quad (2.16)$$

Therefore, in the presence of a QCD axion, the effective $\bar{\theta}$ parameter is nontrivially related to the quark CEDMs \tilde{d}_q and the gluon CEDM w . As discussed later, this relation may be experimentally testable through EDM measurements if the UV contribution $\bar{\theta}_{\text{UV}}$ is subdominant compared to $\bar{\theta}_{\text{BSM}}$. Conversely, EDM data may provide insight into the dominant origin of a nonvanishing axion VEV.

2.2 Renormalization effect

If the operators in Eqs. (2.2)–(2.4) are generated at a high scale well above the QCD scale, they undergo significant mixing through renormalization-group (RG) evolution down to $\mu \sim 1$ GeV. The relevant RG equations are given by [17, 18, 45–47]

$$\frac{d\mathbf{K}}{d\ln\mu} = \frac{g_s^2}{16\pi^2} \gamma \mathbf{K}, \quad (2.17)$$

where $\mathbf{K} \equiv (K_1, K_2, K_3)^T$ with

$$K_1(\mu) = \frac{d_q(\mu)}{m_q Q_q}, \quad K_2(\mu) = \frac{\tilde{d}_q(\mu)}{m_q}, \quad K_3(\mu) = \frac{w(\mu)}{g_s}. \quad (2.18)$$

The anomalous-dimension matrix γ is

$$\gamma = \begin{pmatrix} \gamma_e & \gamma_{eq} & 0 \\ 0 & \gamma_q & \gamma_{Gq} \\ 0 & 0 & \gamma_G \end{pmatrix} = \begin{pmatrix} 8C_F & 8C_F & 0 \\ 0 & 16C_F - 4N_c & -2N_c \\ 0 & 0 & N_c + 2n_f + \beta_0 \end{pmatrix}, \quad (2.19)$$

where $C_F = (N_c^2 - 1)/(2N_c) = 4/3$, $N_c = 3$ is the number of colors, n_f is the number of active light quark flavors with $m_q < \mu$, and $\beta_0 = (33 - 2n_f)/3$.

The strong coupling constant and the quark masses evolve according to

$$\frac{d\alpha_s}{d\ln\mu} = -2\beta_0 \frac{\alpha_s^2}{4\pi}, \quad \frac{dm_q}{d\ln\mu} = -8 \frac{\alpha_s}{4\pi} m_q. \quad (2.20)$$

For renormalization scales $\mu < m_c$ and a BSM scale $\Lambda \geq 1$ TeV at which the CPV operators are generated, analytic solutions to Eq. (2.17) in terms of $g_s(m_q)$ ($q = t, b, c$) are obtained in Ref. [13]. Using numerical values for $g_s(m_q)$, one finds

$$w(1 \text{ GeV}) \simeq 0.33 \left(\frac{g_s(\Lambda)}{g_s(1 \text{ TeV})} \right)^{15/7} w(\Lambda), \quad (2.21)$$

$$\frac{\Delta \tilde{d}_q}{m_q}(1 \text{ GeV}) \simeq \left[0.19 \left(\frac{g_s(\Lambda)}{g_s(1 \text{ TeV})} \right)^{1/3} - 0.06 \left(\frac{g_s(\Lambda)}{g_s(1 \text{ TeV})} \right)^{15/7} \right] w(\Lambda), \quad (2.22)$$

where $\Delta \tilde{d}_q$ denotes the RG-induced contribution to the quark CEDM arising from the gluon CEDM.

Consequently, depending on the scale Λ at which the gluon CEDM is generated,

$$\frac{\Delta \tilde{d}_q}{m_q}(1 \text{ GeV}) = r(\Lambda) w(1 \text{ GeV}), \quad (2.23)$$

with representative values

$$r(\Lambda) \simeq \begin{cases} 0.41, & \Lambda = 1 \text{ TeV}, \\ 0.53, & \Lambda = 10 \text{ TeV}, \\ 0.65, & \Lambda = 100 \text{ TeV}. \end{cases} \quad (2.24)$$

This RG mixing plays an important role in the gluon CEDM contribution to CPV pion–nucleon interactions, which are key ingredients in nuclear and atomic EDMs.

3 CP-odd interactions at IR

The CP-odd operators of the previous section generated at a BSM scale induce CP-odd interactions of hadrons and electrons at low energies below the QCD scale. At leading order, the relevant operators are¹

$$\mathcal{L}_{\text{dipole}} = -\frac{i}{2} \bar{N} \left(d_p \frac{1 + \tau_3}{2} + d_n \frac{1 - \tau_3}{2} \right) \sigma^{\mu\nu} F_{\mu\nu} \gamma_5 N - \frac{i}{2} d_e \bar{e} \sigma^{\mu\nu} F_{\mu\nu} \gamma_5 e, \quad (3.1)$$

$$\mathcal{L}_{\pi N} = \bar{g}_0 \bar{N} \vec{\tau} \cdot \vec{\pi} N + \bar{g}_1 \pi_3 \bar{N} N, \quad (3.2)$$

$$\mathcal{L}_{4N} = C_1 \bar{N} N D_\mu (N^\dagger S^\mu N) + C_2 \bar{N} \vec{\tau} N \cdot D_\mu (N^\dagger \vec{\tau} S^\mu N), \quad (3.3)$$

$$\mathcal{L}_{eN} = -\frac{G_F}{\sqrt{2}} (\bar{e} i \gamma_5 e) \bar{N} (C_S^{(0)} + C_S^{(1)} \tau_3) N, \quad (3.4)$$

where $N = (p \ n)^T$ are the nucleon fields, $\vec{\pi} = (\pi_1, \pi_2, \pi_3)$ are the pion fields, τ_i ($i = 1, 2, 3$) are Pauli matrices in isospin space, σ_i ($i = 1, 2, 3$) are Pauli matrices in spin space, and $S^\mu = (0, \vec{\sigma}/2)$. The EDMs of nucleons and electrons in Eq. (3.1) directly contribute to nuclear, atomic, or molecular EDMs, while the CP-odd interactions in Eqs. (3.2)-(3.4) contribute to the EDMs by polarizing nuclei, atoms, or molecules. We will discuss in details how these CP-odd operators contribute to the EDMs of nuclei, atoms, and molecules in Sec. 4. In this section, let us discuss the connection between these IR CPV operators and the UV CPV operators of Sec. 2.

In Eqs. (3.1)-(3.4) we have nine independent IR CPV parameters which are

$$X_i^{\text{IR}} \in \left\{ d_p, d_n, \bar{g}_0, \bar{g}_1, C_1, C_2, d_e, C_S^{(0)}, C_S^{(1)} \right\}. \quad (3.5)$$

The parameters X_i^{IR} originate from the UV CPV parameters X_i^{UV} in Eq. (2.5), and they are matched at a scale μ^* near the QCD scale ~ 1 GeV by linear relations approximately:

$$X_i^{\text{IR}} = \sum_j M_{ij} X_j^{\text{UV}} \quad \text{at} \quad \mu = \mu^*. \quad (3.6)$$

In the following we discuss the matrix elements M_{ij} and the choice of the matching scale μ^* .

3.1 Nucleon electric dipole moments

The nucleon EDMs d_N ($N = p, n$) can be sizably induced from the non-leptonic sources $X_i^{\text{UV}} \in \{\bar{\theta}, \tilde{d}_q, d_q, w\}$ ($q = u, d, s$) among the parameters in Eq. (2.5). Let us first discuss contributions from $\{\bar{\theta}, \tilde{d}_q, d_q\}$, and then turn to the contribution from w . Here we will largely rely on the calculations using QCD sum rules for nucleon EDMs [48–54].

The nucleon EDMs induced by $\{\bar{\theta}, \tilde{d}_q, d_q\}$ were computed by QCD sum rules in Refs. [48, 49, 51, 52]:

$$d_N(\bar{\theta}, \tilde{d}_q, d_q) = c_N \Theta_N(\bar{\theta}, \tilde{d}_q, d_q), \quad (N = p, n), \quad (3.7)$$

¹In principle, the three-pion operator $\Delta_\pi \pi^0 \pi^+ \pi^-$ can also be included. In our previous analysis [13], however, we found its contribution to nuclear and atomic EDMs to be generally negligible, and we therefore ignore it here. We also neglect the nuclear spin-dependent interactions $\bar{e} \sigma^{\mu\nu} e \bar{N} S_\mu v_\nu N$ and $\bar{e} e \partial^\mu \bar{N} S_\mu N$, since they are typically subleading compared with the nuclear spin-independent interaction $(\bar{e} i \gamma_5 e)(\bar{N} N)$.

where c_N is an overall normalization factor that depends on the single-pole contribution to the two-point correlator of the nucleon interpolating field. The functions Θ_N are given by

$$\begin{aligned}\Theta_p(\bar{\theta}, \tilde{d}_q, d_q) &= \chi m_* \left[(4e_u - e_d) \left(\bar{\theta} - \frac{m_0^2}{2} \frac{\tilde{d}_s}{m_s} \right) + \frac{m_0^2}{2} (\tilde{d}_u - \tilde{d}_d) \left(\frac{4e_u}{m_d} + \frac{e_d}{m_u} \right) \right] \\ &\quad + \frac{1}{8} (2\kappa + \xi) (4e_u \tilde{d}_u - e_d \tilde{d}_d) + (4d_u - d_d), \\ \Theta_n(\bar{\theta}, \tilde{d}_q, d_q) &= \chi m_* \left[(4e_d - e_u) \left(\bar{\theta} - \frac{m_0^2}{2} \frac{\tilde{d}_s}{m_s} \right) + \frac{m_0^2}{2} (\tilde{d}_d - \tilde{d}_u) \left(\frac{4e_d}{m_u} + \frac{e_u}{m_d} \right) \right] \\ &\quad + \frac{1}{8} (2\kappa + \xi) (4e_d \tilde{d}_d - e_u \tilde{d}_u) + (4d_d - d_u),\end{aligned}\tag{3.8}$$

where $m_* \equiv \left(\sum_{q=u,d,s} m_q^{-1} \right)^{-1} \simeq m_u m_d / (m_u + m_d)$ and e_q denotes the electromagnetic charge of the quark q . The expressions involve quark-condensate susceptibilities [49],

$$\begin{aligned}\langle \bar{q} \sigma_{\mu\nu} q \rangle &= e_q \chi F_{\mu\nu} \langle \bar{q} q \rangle, & g_s \langle \bar{q} G_{\mu\nu} q \rangle &= e_q \kappa F_{\mu\nu} \langle \bar{q} q \rangle, \\ g_s \langle \bar{q} G^{\mu\nu} \sigma_{\mu\nu} q \rangle &= m_0^2 \langle \bar{q} q \rangle, & 2g_s \langle \bar{q} \gamma_5 \tilde{G}_{\mu\nu} q \rangle &= i e_q \xi F_{\mu\nu} \langle \bar{q} q \rangle,\end{aligned}\tag{3.9}$$

whose numerical values are taken as²

$$\begin{aligned}\chi &= -5.7(6) \text{ GeV}^{-2}, & m_0^2 &= 0.8(1) \text{ GeV}^2, \\ \kappa &= -0.34(10), & \xi &= -0.74(20).\end{aligned}\tag{3.10}$$

The overall factor c_N in Eq. (3.7) carries a large theoretical uncertainty due to the poorly known single-pole contribution, leading to a range of choice for the Borel mass in the sum-rule analysis. The corresponding uncertainty in nucleon EDMs can exceed 50% [51]. Ref. [55] instead fixes the normalization by matching to lattice results for quark EDM contributions, which have smaller uncertainties; we follow the same strategy here. The quark-EDM contributions to nucleon EDMs have been determined with good accuracy in lattice QCD [57, 58]:

$$\begin{aligned}d_p(d_q) &= g_T^u d_d + g_T^d d_u + g_T^s d_s, \\ d_n(d_q) &= g_T^u d_u + g_T^d d_d + g_T^s d_s,\end{aligned}\tag{3.11}$$

where the tensor charges are³

$$g_T^u = -0.195(16), \quad g_T^d = 0.782(28), \quad g_T^s = -0.0016(12),\tag{3.12}$$

²Ref. [55] adopts smaller values of χ based on a recent lattice determination, by a factor of ~ 3 compared to earlier estimates. As also noted there, there are arguments suggesting that the product $m_0^2 \chi$ is approximately fixed, $m_0^2 \chi \simeq 6$ [56], which supports the original estimate. Further lattice studies are needed; here we use the original value of χ .

³Ref. [59] argues, based on several considerations, that $|g_T^s|$ should be as large as $\mathcal{O}(0.1) |g_T^{u,d}|$ barring accidental cancellations, making questions on both the lattice results for g_T^s and the validity of leading-order QCD sum-rule estimates. In this work we nevertheless adopt the lattice values and leading-order sum-rule expressions. A significantly larger g_T^s could modify our estimates of nuclear and atomic EDMs sourced by quark EDMs.

given at $\mu = 2$ GeV in Ref. [57]. To use these to determine c_N in Eq. (3.7), we evolve the tensor charges to $\mu = 1$ GeV, the matching scale used in Eq. (3.7) above. We find $g_T^q(1 \text{ GeV})/g_T^q(2 \text{ GeV}) \simeq 1.047$, and thus obtain⁴

$$c_N^{\text{lattice}} \simeq -g_T^u(1 \text{ GeV}) = 0.204(17). \quad (3.13)$$

Using this value in Eq. (3.7), we obtain⁵

$$d_p = -1.16(16) \cdot 10^{-16} \bar{\theta} e \text{ cm} + e \left(-0.38(6) \tilde{d}_u + 0.27(5) \tilde{d}_d + 0.022(4) \tilde{d}_s \right) + 0.82(7) d_u - 0.204(17) d_d, \quad (3.14)$$

$$d_n = 0.77(10) \cdot 10^{-16} \bar{\theta} e \text{ cm} + e \left(-0.30(6) \tilde{d}_u + 0.37(6) \tilde{d}_d - 0.0145(27) \tilde{d}_s \right) - 0.204(17) d_u + 0.82(7) d_d. \quad (3.15)$$

Assuming $\tilde{d}_s = (m_s/m_d) \tilde{d}_d$ as discussed around Eq. (2.6), the above equations become

$$d_p = -1.16(16) \cdot 10^{-16} \bar{\theta} e \text{ cm} + e \left(-0.38(6) \tilde{d}_u + 0.70(9) \tilde{d}_d \right) + 0.82(7) d_u - 0.204(17) d_d, \quad (3.16)$$

$$d_n = 0.77(10) \cdot 10^{-16} \bar{\theta} e \text{ cm} + e \left(-0.30(6) \tilde{d}_u + 0.08(8) \tilde{d}_d \right) - 0.204(17) d_u + 0.82(7) d_d. \quad (3.17)$$

Here we note that $\partial d_n / \partial \tilde{d}_d$ becomes significantly smaller than $\partial d_p / \partial \tilde{d}_d$, due to an accidental cancellation between the down- and strange-quark CEDM contributions to d_n under the relation $\tilde{d}_s = (m_s/m_d) \tilde{d}_d$.

If the PQ mechanism for the strong CP problem is realized, leading to Eq. (2.16), one finds

$$\begin{aligned} \Theta_p^{\text{PQ}}(\bar{\theta}_{\text{UV}}, \tilde{d}_q, d_q) &= \chi m_* (4e_u - e_d) \bar{\theta}_{\text{UV}} + \left(\frac{1}{8}(2\kappa + \xi) + \frac{1}{2} \chi m_0^2 \right) (4e_u \tilde{d}_u - e_d \tilde{d}_d) + (4d_u - d_d), \\ \Theta_n^{\text{PQ}}(\bar{\theta}_{\text{UV}}, \tilde{d}_q, d_q) &= \chi m_* (4e_d - e_u) \bar{\theta}_{\text{UV}} + \left(\frac{1}{8}(2\kappa + \xi) + \frac{1}{2} \chi m_0^2 \right) (4e_d \tilde{d}_d - e_u \tilde{d}_u) + (4d_d - d_u), \end{aligned} \quad (3.18)$$

where the strange-quark contribution cancels exactly against $\bar{\theta}_{\text{BSM}}$ in Eq. (2.13). Numerically,

$$d_p^{\text{PQ}} = -1.16(16) \cdot 10^{-16} \bar{\theta}_{\text{UV}} e \text{ cm} + e \left(-1.34(23) \tilde{d}_u - 0.167(29) \tilde{d}_d \right) + 0.82(7) d_u - 0.204(17) d_d, \quad (3.19)$$

$$d_n^{\text{PQ}} = 0.77(10) \cdot 10^{-16} \bar{\theta}_{\text{UV}} e \text{ cm} + e \left(0.33(6) \tilde{d}_u + 0.67(12) \tilde{d}_d \right) - 0.204(17) d_u + 0.82(7) d_d. \quad (3.20)$$

⁴One may alternatively take $c_N^{\text{lattice}} \simeq \frac{1}{4} g_T^d(1 \text{ GeV}) = 0.205(7)$, which has a smaller uncertainty. To be conservative, we choose g_T^u instead.

⁵We use the $\overline{\text{MS}}$ quark masses in Ref. [60]: $m_u = 2.16(7)$ MeV, $m_d = 4.70(7)$ MeV, and $m_s = 93.5(8)$ MeV at $\mu = 2$ GeV. We evolve them to $\mu = 1$ GeV using one-loop QCD running, which gives $m_q(1 \text{ GeV}) \simeq 1.15 m_q(2 \text{ GeV})$.

In the leading sum-rule expressions of Eq. (3.8) and Eq. (3.18), one can observe that the dependence on the quark-condensate susceptibilities largely cancels in the EDM ratio d_p/d_n . Moreover, the ratio does not depend on the normalization factor c_N . Within the QCD sum-rule approach, therefore, the EDM ratio d_p/d_n is predicted quite precisely. If the nucleon EDMs are dominantly from $\bar{\theta}$, the ratio is

$$\frac{d_p(\bar{\theta})}{d_n(\bar{\theta})} = \frac{d_p^{\text{PQ}}(\bar{\theta}_{\text{UV}})}{d_n^{\text{PQ}}(\bar{\theta}_{\text{UV}})} = \frac{4e_u - e_d + \dots}{4e_d - e_u + \dots} = -\frac{3}{2}(1 \pm \mathcal{O}(0.1)). \quad (3.21)$$

where the ellipsis denotes the higher-order contributions in the operator product expansion (OPE) of the sum rule, which is estimated to be $\mathcal{O}(10)\%$ [51]. In the case that the nucleon EDMs are dominantly from quark CEDMs \tilde{d}_q , assuming the relation $\tilde{d}_s = (m_s/m_d)\tilde{d}_d$ in Eq. (2.6),

$$\begin{aligned} \frac{d_p(\tilde{d}_q)}{d_n(\tilde{d}_q)} &= \frac{\left(m_* \left(\frac{4e_u}{m_d} + \frac{e_d}{m_u}\right) + e_u \zeta\right) \tilde{d}_u - \left(m_* \left(\frac{8e_u - e_d}{m_d} + \frac{e_d}{m_u}\right) + \frac{e_d}{4} \zeta\right) \tilde{d}_d + \dots}{-\left(m_* \left(\frac{4e_d}{m_u} + \frac{e_u}{m_d}\right) + \frac{e_u}{4} \zeta\right) \tilde{d}_u + \left(m_* \left(\frac{4e_d}{m_u} + \frac{2e_u - 4e_d}{m_d}\right) + e_d \zeta\right) \tilde{d}_d + \dots}, \\ &\simeq \frac{0.81(6)\tilde{d}_u - 1.51(4)\tilde{d}_d}{0.64(4)\tilde{d}_u - 0.18(4)\tilde{d}_d} (1 \pm \mathcal{O}(0.1)), \end{aligned} \quad (3.22)$$

where $\zeta \equiv (2\kappa + \xi)/(m_0^2\chi) \simeq 0.31(8)$, and the ellipsis again denotes the higher-order contributions in the OPE accounted for by the factor $(1 \pm \mathcal{O}(0.1))$ in the last expression. We again note that $\partial d_n/\partial \tilde{d}_d$ is suppressed relative to $\partial d_p/\partial \tilde{d}_d$ by about an order of magnitude, since

$$\left(\frac{4e_d}{m_u} + \frac{2e_u - 4e_d}{m_d}\right) \propto (m_d - 2m_u) \approx 0. \quad (3.23)$$

This suppression originates from an accidental cancellation between the down- and strange-quark contributions to d_n under the relation $\tilde{d}_s = (m_s/m_d)\tilde{d}_d$. In the presence of the PQ mechanism, the proton-to-neutron EDM ratio induced by quark CEDMs can be significantly modified:

$$\frac{d_p^{\text{PQ}}(\tilde{d}_q)}{d_n^{\text{PQ}}(\tilde{d}_q)} = -\frac{4e_u \tilde{d}_u - e_d \tilde{d}_d + \dots}{e_u \tilde{d}_u - 4e_d \tilde{d}_d + \dots} = -\frac{8\tilde{d}_u + \tilde{d}_d}{2\tilde{d}_u + 4\tilde{d}_d} (1 \pm \mathcal{O}(0.1)). \quad (3.24)$$

Finally, if the dominant UV CPV source is quark EDMs d_q , the ratio turns out to be

$$\frac{d_p(d_q)}{d_n(d_q)} = \frac{d_p^{\text{PQ}}(d_q)}{d_n^{\text{PQ}}(d_q)} = -\frac{4d_u - d_d}{d_u - 4d_d} (1 \pm \mathcal{O}(0.1)) \quad (3.25)$$

with the higher-order contributions of the OPE estimated as $\mathcal{O}(10)\%$ [51].

Let us now discuss the contribution of the gluon CEDM (or Weinberg three-gluon operator) to nucleon EDMs. Since the gluon CEDM does not break the chiral symmetry, it turns out that the one-particle reducible contribution from the CP-odd nucleon mass is comparable to the one-particle irreducible contribution unlike the QCD θ -term or quark

CEDMs [61, 62]. Therefore, the total contribution has been computed as a sum of the two parts:

$$d_N(w) = d_N^{(\text{red})}(w) + d_N^{(\text{irr})}(w). \quad (3.26)$$

The reducible contribution is obtained by the chiral rotation of the anomalous magnetic moment with the CP-odd nucleon mass that can be evaluated using QCD sum rules [50, 53]:

$$d_N^{(\text{red})}(w) = -\mu_N^{\text{an}} \frac{3g_s m_0^2}{32\pi^2} w \ln\left(\frac{M^2}{\mu_{\text{IR}}^2}\right), \quad (3.27)$$

where μ_N^{an} is the nucleon anomalous magnetic moment, g_s and w are evaluated at $\mu = 1$ GeV, M is the Borel mass, and μ_{IR} is an IR cutoff in the sum-rule analysis. The dominant uncertainty arises from m_0^2 and the range of M/μ_{IR} , taken as $\sqrt{2} \leq M/\mu_{\text{IR}} \leq 2\sqrt{2}$ [53], yielding

$$d_p^{(\text{red})}(w) = -23(11) w e \text{ MeV}, \quad (3.28)$$

$$d_n^{(\text{red})}(w) = 25(11) w e \text{ MeV}. \quad (3.29)$$

On the other hand, the irreducible contribution is estimated in Ref. [54] using a nonrelativistic quark model:

$$d_p^{(\text{irr})}(w) = 4.5(5) w e \text{ MeV}, \quad (3.30)$$

$$d_n^{(\text{irr})}(w) = -4.5(5) w e \text{ MeV}, \quad (3.31)$$

where the uncertainty reflects model-dependent choices for the quark interaction. Combining the two contributions gives, at $\mu = 1$ GeV,

$$d_p(w) = -19(11) w e \text{ MeV}, \quad (3.32)$$

$$d_n(w) = 20(11) w e \text{ MeV}. \quad (3.33)$$

Although the absolute normalization carries an $\mathcal{O}(50\%)$ uncertainty, the ratio is significantly more robust within this framework:

$$\frac{d_p(w)}{d_n(w)} = -0.90(3). \quad (3.34)$$

Finally we remark that the PQ mechanism would make a negligible change for the nucleon EDMs from the gluon CEDM, unlike the quark CEDMs, if the shifted axion VEV from the gluon CEDM does not significantly differ from the NDA estimation in Eq. (2.13).

3.2 CP-odd pion-nucleon interactions

The CP-odd pion–nucleon couplings \bar{g}_0 and \bar{g}_1 in Eq. (3.2) can receive sizable contributions from purely hadronic UV sources $X_i^{\text{UV}} \in \{\bar{\theta}, \tilde{d}_q, w\}$ with $q = u, d, s$. The state-of-the-art results for these couplings are summarized in detail in Ref. [13]. Here we briefly present the essential formulas.

The couplings \bar{g}_0 and \bar{g}_1 induced by the QCD θ term can be computed in chiral perturbation theory in terms of quark-mass contributions to baryon masses [63, 64]⁶:

$$\bar{g}_0(\bar{\theta}) = \frac{\delta m_N}{2f_\pi} \frac{1 - \epsilon^2}{2\epsilon} \bar{\theta} = 15.7(1.7) \times 10^{-3} \bar{\theta}, \quad (3.35)$$

$$\bar{g}_1(\bar{\theta}) = \left(8c_1 m_N \frac{\epsilon(1 - \epsilon^2)}{16f_\pi m_N} \frac{m_\pi^4}{m_K^2 - m_\pi^2} + \mathcal{O}\left(\epsilon \frac{m_\pi^4}{m_N^3 f_\pi}\right) \right) \bar{\theta} = -3.4(2.4) \times 10^{-3} \bar{\theta}, \quad (3.36)$$

where $\delta m_N = m_n - m_p = 2.49(17)$ MeV, $\epsilon = (m_d - m_u)/(2\bar{m}) = 0.37(3)$, $\bar{m} = (m_u + m_d)/2 = 3.37(8)$ MeV, $c_1 = 1.0(3)$ GeV⁻¹ is related to the nucleon sigma term as $\sigma_{\pi N} = -4c_1 m_\pi^2 + \mathcal{O}(m_\pi^3)$ [66, 67], $f_\pi = 92.2$ MeV, $m_K = 495$ MeV, and $m_\pi = 135$ MeV.

The contributions from quark CEDMs were first computed using QCD sum rules [68] and have recently been refined within chiral perturbation theory [12], building on the observation of Ref. [69].⁷ The resulting expressions are

$$\begin{aligned} \bar{g}_0(\tilde{d}_q) &\simeq \frac{m_0^2}{8f_\pi} \left[\delta_{g_0} \frac{d\delta m_N}{d(\bar{m}\epsilon)} (\tilde{d}_u + \tilde{d}_d) - \frac{(1 - \epsilon^2)\delta m_N}{\epsilon} \sum_{q=u,d,s} \frac{\tilde{d}_q}{m_q} \right], \\ &\simeq -0.4(0.9) \tilde{d}_u \text{ GeV} + 1.0(0.8) \tilde{d}_d \text{ GeV} - 0.059(10) \tilde{d}_s \text{ GeV}, \quad (3.37) \\ &\simeq -0.4(0.9) \tilde{d}_u \text{ GeV} - 0.2(0.8) \tilde{d}_d \text{ GeV} \quad (\text{for } \tilde{d}_s = (m_s/m_d)\tilde{d}_d), \quad (3.38) \end{aligned}$$

$$\bar{g}_0^{\text{PQ}}(\tilde{d}_q) \simeq \delta_{g_0} \frac{m_0^2}{8f_\pi} \frac{d\delta m_N}{d(\bar{m}\epsilon)} (\tilde{d}_u + \tilde{d}_d) \simeq 2.2(0.7) (\tilde{d}_u + \tilde{d}_d) \text{ GeV}, \quad (3.39)$$

$$\bar{g}_1(\tilde{d}_q) \simeq \bar{g}_1^{\text{PQ}}(\tilde{d}_q) \simeq \delta_{g_1} \frac{1}{2f_\pi} (\tilde{d}_u - \tilde{d}_d) \frac{m_0^2}{2} \frac{\sigma_{\pi N}}{\bar{m}} = 38(13) (\tilde{d}_u - \tilde{d}_d) \text{ GeV}, \quad (3.40)$$

evaluated at the matching scale $\mu = 1$ GeV. Here $d\delta m_N/d(\bar{m}\epsilon) \simeq \delta m_N/(\bar{m}\epsilon)$, $\sigma_{\pi N} = 59.1(3.5)$ MeV, and $\delta_{g_0, g_1} = 1.0 \pm 0.3$ account for theoretical uncertainties. The superscript ‘‘PQ’’ in Eqs. (3.39) and (3.40) denotes the couplings in the presence of the PQ mechanism, including the effect of the shifted axion VEV in Eq. (2.13).

Lastly, the contribution of the gluon CEDM to the coupling \bar{g}_1 has been computed using chiral perturbation theory combined with QCD sum rules in Ref. [71]:

$$\bar{g}_1(w) \simeq \bar{g}_1^{\text{PQ}}(w) \simeq \langle 0 | \mathcal{L}_w | \pi^0 \rangle \left(\frac{\sigma_{\pi N}}{f_\pi^2 m_\pi^2} + \frac{5g_A^2 m_\pi}{64\pi f_\pi^4} \right) \simeq \pm(2.6 \pm 1.5) \times 10^{-3} w \text{ GeV}^2, \quad (3.41)$$

evaluated at the matching scale $\mu = 1$ GeV. Here $\mathcal{L}_w = \frac{1}{3} w f^{abc} G_\alpha^{a\mu} G_\mu^{b\delta} \tilde{G}_\delta^{c\alpha}$ denotes the Weinberg three-gluon operator (i.e. the gluon CEDM), and $g_A = 1.27$ is the nucleon axial-

⁶For comparison, see also large- N_c estimation in [65] which shows good agreement with previous results.

⁷Recently, Ref. [70] revisited the observation made in Ref. [69] and pointed out that the nucleon form factors neglected in Ref. [69] may not be small, based on large- N_c arguments. Estimating these form factors using large- N_c scaling with $N_c = 3$ suggests that the previous estimates of $g_0(\tilde{d}_q)$ and $g_1(\tilde{d}_q)$ in Refs. [12, 69] may receive sizable corrections. We find that, under this rough $N_c = 3$ estimate, the corrections can exceed 100% for $\bar{g}_0(\tilde{d}_q)$ and amount to about 70% for $\bar{g}_1(\tilde{d}_q)$. However, since these form factors are currently unknown apart from such large- N_c estimates, we do not include these potential contributions in this work. For the analysis in Sec. 5, the omitted contributions could approximately double the error bars of the predicted EDM ratios sourced by \tilde{d}_q , mainly due to the increased uncertainty in $\bar{g}_1(\tilde{d}_q)$, while the impact of $\bar{g}_0(\tilde{d}_q)$ remains small.

vector coupling. The sign ambiguity arises from the QCD sum-rule estimate of the matrix element of the Weinberg operator.

On the other hand, there is no dedicated computation of $\bar{g}_0(w)$ to date. Applying naive dimensional analysis (NDA), we estimate

$$\bar{g}_0(w) \sim \bar{g}_0^{\text{PQ}}(w) \sim (m_u + m_d)|_{\mu_{\text{NDA}}} \Lambda_\chi w|_{\mu_{\text{NDA}}} \sim 9 \times 10^{-3} w|_{1 \text{ GeV}} \text{ GeV}^2, \quad (3.42)$$

where $\mu_{\text{NDA}} \simeq 225 \text{ MeV}$ is the NDA matching scale defined by $\alpha_s(\mu_{\text{NDA}})/(4\pi) \simeq 1/6$, at which the QCD one-loop beta function becomes comparable to the two-loop contribution [72]. The final expression is obtained by evolving the parameters to $\mu = 1 \text{ GeV}$ for comparison with quantities evaluated using QCD sum rules.

If the gluon CEDM is generated at a high scale, the quark CEDMs induced through RG mixing (cf. Eq. (2.22)) can provide an important contribution. Using Eq. (2.23), we obtain

$$\bar{g}_1(\Delta\tilde{d}_q) \simeq \bar{g}_1^{\text{PQ}}(\Delta\tilde{d}_q) \simeq -0.11(4) r(\Lambda) w \text{ GeV}^2, \quad (3.43)$$

$$\bar{g}_0(\Delta\tilde{d}_q) \simeq -2(6) \times 10^{-3} r(\Lambda) w \text{ GeV}^2, \quad (3.44)$$

$$\bar{g}_0^{\text{PQ}}(\Delta\tilde{d}_q) \simeq 17(6) \times 10^{-3} r(\Lambda) w \text{ GeV}^2, \quad (3.45)$$

where $\Delta\tilde{d}_q$ denotes the RG-induced quark CEDM generated from a gluon CEDM at the scale Λ , and w is renormalized at $\mu = 1 \text{ GeV}$. For $\Lambda \gtrsim 1 \text{ TeV}$, one typically has $r(\Lambda) = \mathcal{O}(1)$ (see Eq. (2.24)). It then follows that

$$\bar{g}_1^{(\text{PQ})}(\Delta\tilde{d}_q) \gg \bar{g}_1^{(\text{PQ})}(w) \sim \bar{g}_0^{(\text{PQ})}(w) \sim \bar{g}_0^{(\text{PQ})}(\Delta\tilde{d}_q), \quad (3.46)$$

at $\mu = 1 \text{ GeV}$ for $\Lambda \gtrsim 1 \text{ TeV}$, where $\bar{g}_{0,1}^{(\text{PQ})}(w)$ denote the direct contributions of w in Eqs. (3.41) and (3.42). This implies that the CP-odd pion–nucleon couplings $\bar{g}_{0,1}$ induced by a gluon CEDM generated at $\Lambda \gtrsim 1 \text{ TeV}$ are dominated by the contributions arising from RG-induced quark CEDMs at $\mu \sim 1 \text{ GeV}$.

We now consider the ratios $e\bar{g}_0/(\Lambda_\chi d_n)$ and $e\bar{g}_1/(\Lambda_\chi d_n)$, which are useful for assessing the relative sizes of nuclear and atomic EDMs with respect to the neutron EDM. Throughout, we assume $\tilde{d}_s = (m_s/m_d)\tilde{d}_d$, as in Eq. (2.6).

If the QCD θ term is the dominant CPV source, we find

$$\frac{e\bar{g}_0(\bar{\theta})}{\Lambda_\chi d_n(\bar{\theta})} = \frac{e\bar{g}_0^{\text{PQ}}(\bar{\theta}_{\text{UV}})}{\Lambda_\chi d_n^{\text{PQ}}(\bar{\theta}_{\text{UV}})} (\sim 4\pi)_{\text{NDA}} \simeq 3.5(6), \quad (3.47)$$

$$\frac{e\bar{g}_1(\bar{\theta})}{\Lambda_\chi d_n(\bar{\theta})} = \frac{e\bar{g}_1^{\text{PQ}}(\bar{\theta}_{\text{UV}})}{\Lambda_\chi d_n^{\text{PQ}}(\bar{\theta}_{\text{UV}})} \left(\sim 4\pi \frac{m_u - m_d}{m_s} \right)_{\text{NDA}} \simeq -0.8(5), \quad (3.48)$$

where the NDA estimates are shown in parentheses (see Appendix for details).

For quark CEDMs, we obtain

$$\frac{e\bar{g}_0(\tilde{d}_q)}{\Lambda_\chi d_n(\tilde{d}_q)} (\sim 4\pi)_{\text{NDA}} \simeq \frac{4(11)\tilde{d}_u + 2(10)\tilde{d}_d}{4.4(8)\tilde{d}_u - 1.2(11)\tilde{d}_d}, \quad (3.49)$$

$$\frac{e\bar{g}_0^{\text{PQ}}(\tilde{d}_q)}{\Lambda_\chi d_n^{\text{PQ}}(\tilde{d}_q)} \left(\sim 4\pi \frac{\tilde{d}_u + \tilde{d}_d}{\tilde{d}_q} \right)_{\text{NDA}} \simeq \frac{5.6(2.2)(\tilde{d}_u + \tilde{d}_d)}{\tilde{d}_u + 2\tilde{d}_d}, \quad (3.50)$$

$$\frac{e\bar{g}_1(\tilde{d}_q)}{\Lambda_\chi d_n(\tilde{d}_q)} \left(\sim 4\pi \frac{\tilde{d}_u - \tilde{d}_d}{\tilde{d}_q} \right)_{\text{NDA}} \simeq \frac{-483(165)(\tilde{d}_u - \tilde{d}_d)}{4.4(8)\tilde{d}_u - 1.2(11)\tilde{d}_d}, \quad (3.51)$$

$$\frac{e\bar{g}_1^{\text{PQ}}(\tilde{d}_q)}{\Lambda_\chi d_n^{\text{PQ}}(\tilde{d}_q)} \left(\sim 4\pi \frac{\tilde{d}_u - \tilde{d}_d}{\tilde{d}_q} \right)_{\text{NDA}} \simeq \frac{99(37)(\tilde{d}_u - \tilde{d}_d)}{\tilde{d}_u + 2\tilde{d}_d}. \quad (3.52)$$

If the dominant CPV source is a gluon CEDM generated at Λ , we obtain

$$\frac{e\bar{g}_0(w)}{\Lambda_\chi d_n(w)} \simeq -0.08(28) r(\Lambda) \pm \frac{m_u + m_d}{f_\pi}, \quad (3.53)$$

$$\frac{e\bar{g}_0^{\text{PQ}}(w)}{\Lambda_\chi d_n^{\text{PQ}}(w)} \simeq 0.7(5) r(\Lambda) \pm \frac{m_u + m_d}{f_\pi}, \quad (3.54)$$

$$\frac{e\bar{g}_1(w)}{\Lambda_\chi d_n(w)} \simeq \frac{e\bar{g}_1^{\text{PQ}}(w)}{\Lambda_\chi d_n^{\text{PQ}}(w)} \simeq -4.8(3.3) r(\Lambda) \pm 0.11(9), \quad (3.55)$$

where the terms proportional to $r(\Lambda)$ arise from the RG-induced quark CEDMs.

3.3 CP-odd four-nucleon contact interactions

The CP-odd four-nucleon couplings C_1 and C_2 in Eq. (3.3) contribute to nuclear and atomic EDMs by inducing nuclear polarization through CP-odd nuclear forces. Their relative importance can be assessed by comparing the short-range contact CP-odd nuclear force generated by $C_{1,2}$ with the pion-exchange CP-odd nuclear force induced by $\bar{g}_{0,1}$. From a comparison of the corresponding tree-level diagrams, one finds that the contact contribution can dominate over the pion-exchange contribution only if

$$C_{1,2} \gtrsim \frac{\bar{g}_{0,1}}{m_\pi^2 \Lambda_\chi} \sim \bar{g}_{0,1} \text{ fm}^3. \quad (3.56)$$

As discussed in Ref. [13], naive dimensional analysis (NDA) indicates that this condition can be satisfied only if the dominant CP-violating (CPV) source is the gluon CEDM among the hadronic UV sources $X_i^{\text{UV}} \in \{\bar{\theta}, \tilde{d}_q, w\}$. The underlying reason is that the gluon CEDM preserves light-quark chiral symmetry, so that $C_{1,2}(w)$ are not suppressed by light-quark masses, whereas the QCD θ term and quark CEDMs break chiral symmetry and therefore lead to such suppressions. Therefore, within NDA, the contributions of $C_{1,2}$ to nuclear and atomic EDMs need to be included only if the dominant CPV source involves the gluon CEDM.

The calculation of C_1 induced by the gluon CEDM beyond NDA has been performed in Ref. [73] using non-relativistic quark models. The result is

$$C_1(w) = 0.3_{-1.3}^{+5} w \text{ GeV}^{-1}, \quad (3.57)$$

evaluated at the matching scale $\mu = 1$ GeV. On the other hand, there is as yet no calculation of $C_2(w)$ beyond NDA. Nevertheless, $C_2(w)$ may be negligible compared to $C_1(w)$ if their relative sizes follow those of their CP-even counterparts:

$$\mathcal{L}_{NNNN} = -\frac{1}{2}k_S \bar{N}N\bar{N}N + 2k_T \bar{N}\vec{\sigma}N \cdot \bar{N}\vec{\sigma}N. \quad (3.58)$$

It is well known that the CP-even couplings are $k_S = -120.8 \text{ GeV}^{-2}$ and $k_T = 1.8 \text{ GeV}^{-2}$ [74]. The corresponding CP-odd couplings are given by ⁸

$$\bar{k}_S = m_N(C_1 - 2C_2), \quad \bar{k}_T = \frac{1}{4}m_N C_2, \quad (3.61)$$

which implies $|C_2| \ll |C_1|$ if $|\bar{k}_T| \ll |\bar{k}_S|$.

Finally, we estimate the ratio $ef_\pi^2 C_1(w)/d_n(w)$, which will be useful in Sec. 5:

$$\frac{ef_\pi^2 C_1(w)}{d_n(w)} (\sim 1)_{\text{NDA}} = 0.1_{-0.6}^{+2.1}. \quad (3.62)$$

3.4 Semi-leptonic interactions

The semi-leptonic CP-odd couplings $C_S^{(0)}$ and $C_S^{(1)}$ in Eq. (3.4) contribute to atomic and molecular EDMs by inducing polarization of the systems. Their effects are proportional to the nucleon-averaged coupling C_S for a given nucleus:

$$C_S \equiv \frac{Z}{A}C_S^{(p)} + \frac{N}{A}C_S^{(n)} = C_S^{(0)} + \frac{Z-N}{A}C_S^{(1)}, \quad (3.63)$$

where $C_S^{(p)} = C_S^{(0)} + C_S^{(1)}$, $C_S^{(n)} = C_S^{(0)} - C_S^{(1)}$, Z is the proton number, N is the neutron number, and $A = Z + N$ is the mass number.

These semi-leptonic CP-odd couplings can dominantly arise from the CP-odd electron-down-quark interaction $\text{Im}(C_{eeDD})$ in Eq. (2.5):

$$C_S^{(0)} = -g_S^{(0)} \text{Im}(C_{eeDD}), \quad C_S^{(1)} = g_S^{(1)} \text{Im}(C_{eeDD}), \quad (3.64)$$

where $g_S^{(0)}$ and $g_S^{(1)}$ are determined by nucleon matrix elements of light-quark bilinears,

$$g_S^{(0)} = \frac{1}{2} \langle N | \bar{u}u + \bar{d}d | N \rangle, \quad g_S^{(1)} = \frac{1}{2} \langle N | \bar{u}u - \bar{d}d | N \rangle. \quad (3.65)$$

Since $g_S^{(1)} \sim \mathcal{O}(0.1)g_S^{(0)}$ and $(Z-N)/A \simeq -0.2$ with only small variations of order ± 0.03 across paramagnetic systems relevant for EDM experiments (see Sec. 4), the combination $C_S = C_S^{(0)} + \frac{Z-N}{A}C_S^{(1)}$ is nearly constant across different atoms and molecules.

⁸The non-relativistic Lagrangian (3.3) can be derived from the relativistic Lagrangian

$$\mathcal{L}_{4N} = -\frac{m_N}{2} [C_1 \bar{N}N\bar{N}i\gamma_5 N + C_2 \bar{N}\vec{\tau}N \cdot \bar{N}\vec{\tau}i\gamma_5 N], \quad (3.59)$$

which, using Fierz identities, can be rewritten as

$$\mathcal{L}_{4N} = -\frac{m_N}{2} [(C_1 - 2C_2)\bar{N}N\bar{N}i\gamma_5 N - C_2 \bar{N}\vec{\sigma}N \cdot \bar{N}\vec{\sigma}i\gamma_5 N]. \quad (3.60)$$

On the other hand, C_S can also receive sizable contributions from long-distance hadronic interactions induced by $\bar{g}_{0,1}$ and d_N , as discussed in [75–77]. We denote this contribution as C_S^{IR} . The result of Ref. [75] can be written as

$$\frac{G_F}{\sqrt{2}} C_S^{\text{IR}}(\bar{g}_0, \bar{g}_1, d_p, d_n) = - \left(\frac{Z}{A} \xi_p + \frac{N}{A} \xi_n \right) \frac{3\alpha m_e}{2\pi} + \left(\frac{Z}{A} \frac{\mu_p}{\mu_N} \frac{d_p}{e} + \frac{N}{A} \frac{\mu_n}{\mu_N} \frac{d_n}{e} \right) \frac{8\alpha^2 m_e}{m_N p_F} \ln A, \quad (3.66)$$

where $\mu_{p,n}$ are the nucleon magnetic dipole moments, μ_N is the nuclear magneton, and $p_F \simeq 250$ MeV is the nuclear Fermi momentum. The coefficients $\xi_{p,n}$ are given by

$$\begin{aligned} \xi_p &\simeq - \frac{\alpha}{\pi f_\pi m_{\pi^0}^2} \left[(\bar{g}_1 + \bar{g}_0) \ln \frac{m_\rho}{m_e} + \frac{\bar{g}_0^{\eta NN}}{\sqrt{3}} \frac{m_{\pi^0}^2}{m_\eta^2} \frac{f_\pi}{f_\eta} \ln \frac{m_\rho}{m_e} \right] \\ &\quad - \frac{\alpha g_A}{6 f_\pi m_{\pi^\pm} m_N} \frac{\mu_n}{\mu_N} \bar{g}_0 \left(\ln \frac{m_{\pi^\pm}}{m_e} + 1.77 \right), \\ \xi_n &\simeq - \frac{\alpha}{\pi f_\pi m_{\pi^0}^2} \left[(\bar{g}_1 - \bar{g}_0) \ln \frac{m_\rho}{m_e} + \frac{\bar{g}_0^{\eta NN}}{\sqrt{3}} \frac{m_{\pi^0}^2}{m_\eta^2} \frac{f_\pi}{f_\eta} \ln \frac{m_\rho}{m_e} \right] \\ &\quad + \frac{\alpha g_A}{6 f_\pi m_{\pi^\pm} m_N} \frac{\mu_p}{\mu_N} \bar{g}_0 \left(\ln \frac{m_{\pi^\pm}}{m_e} + 1.77 \right), \end{aligned} \quad (3.67)$$

where $g_A = 1.27$ is the nucleon axial-vector coupling, and we use the improved result of Ref. [76] by full two loop computations for the charged pion loop contributions involving $\ln(m_{\pi^\pm}/m_e)$.⁹ For C_S^{IR} arising from the nucleon EDMs (d_p, d_n) in Eq. (3.66), we use the result of Ref. [75], which is based on a simple non-interacting Fermi-gas model of the nucleus. We note, however, that Ref. [77] provides a more dedicated computation of $C_S^{\text{IR}}(d_p, d_n)$ using nuclear matrix elements and shell-model calculations.

For heavy nuclei with $A \sim 200$ and $Z/A \simeq 0.4$, Eq. (3.66) yields

$$C_S^{\text{IR}}(\bar{g}_0, \bar{g}_1, d_p, d_n) \simeq -0.55 \bar{g}_0 + 2.2 \bar{g}_1 + 3.4 \frac{d_p}{e \text{ fm}} - 3.5 \frac{d_n}{e \text{ fm}}, \quad (3.68)$$

where the coefficients vary by less than 10% across the paramagnetic molecules used in EDM experiments.

4 Electric dipole moments of nuclei, atoms, and molecules

In this section, we discuss EDMs of nuclei, atoms, and molecules induced by the IR CP-violating (CPV) parameters introduced in the previous section. We summarize the current theoretical computations for selected light nuclei, atoms, and molecules whose EDMs are being measured or targeted in ongoing and future experiments. At leading order, the EDM d_i of a system i is linearly related to the IR CPV parameters as

$$d_i = \sum_j P_{ij} X_j^{\text{IR}}, \quad (4.1)$$

⁹Compared with Ref. [75], it has an overall factor 2/3 and the extra term +1.77 which amounts to 30% correction to the logarithmic term.

where X_j^{IR} is defined in Eq. (3.5). In the following, we summarize the corresponding matrix elements P_{ij} .

4.1 Light nuclei and diamagnetic atoms

The EDMs of charged light nuclei such as the proton, deuteron (D), and helion (${}^3\text{He}^{++}$) can be directly measured in storage ring experiments [22, 78]. Currently, a precursor storage-ring EDM experiment is underway at COSY by the JEDI collaboration, targeting the deuteron EDM using a magnetic ring [79, 80]. Future electric and magnetic storage-ring experiments are expected to probe the EDMs of such charged light nuclei down to the level of $10^{-29} e \text{ cm}$ [22].

Since light nuclei are relatively simple systems composed of a few nucleons, theoretical calculations of their EDMs in terms of the IR CPV parameters carry uncertainties at the level of $\lesssim 50\%$. In the following, we use the results of Ref. [63]:

$$d_D = 0.94(1) (d_n + d_p) + 0.18(2) \bar{g}_1 e \text{ fm}, \quad (4.2)$$

$$d_{\text{He}} = 0.9 d_n - 0.03(1) d_p + \left[0.11(1) \bar{g}_0 + 0.14(2) \bar{g}_1 - (0.04(2) C_1 - 0.09(2) C_2) \text{ fm}^{-3} \right] e \text{ fm}. \quad (4.3)$$

On the other hand, strong experimental bounds already exist for neutral diamagnetic atoms with heavy nuclei, such as ${}^{199}\text{Hg}$, ${}^{129}\text{Xe}$, ${}^{171}\text{Yb}$, and ${}^{225}\text{Ra}$, obtained using atomic spin-precession spectroscopy. We summarize the current best limits on EDMs of various systems in Table 1. For a comprehensive overview of the experimental status, see Ref. [8].

For the matrix elements in Eq. (4.1), we adopt the summary given in Table 5 of Ref. [8], which is based on Refs. [81, 82] for ${}^{199}\text{Hg}$, Refs. [81, 83] for ${}^{129}\text{Xe}$, Refs. [84–86] for ${}^{171}\text{Yb}$, and Refs. [6, 84, 85] for ${}^{225}\text{Ra}$. In addition, we update the coefficients of \bar{g}_0 , \bar{g}_1 , C_1 , and C_2 for ${}^{225}\text{Ra}$ using Ref. [87]. The resulting EDMs are

$$d_{\text{Hg}} = -2.26(23) \cdot 10^{-4} \left[0.6_{-0.12}^{+1.33} d_n + 0.06_{-0.01}^{+0.20} d_p + \frac{g^{AmN}}{f_\pi} (0.01_{-0.005}^{+0.04} \bar{g}_0 + 0.02_{-0.05}^{+0.07} \bar{g}_1) e \text{ fm} \right], \quad (4.4)$$

$$d_{\text{Xe}} = 3.62(25) \cdot 10^{-5} \left[0.63_{-0.12}^{+0.16} d_n + 0.14(3) d_p + \frac{g^{AmN}}{f_\pi} (-0.008_{-0.042}^{+0.003} \bar{g}_0 + 0.006_{-0.003}^{+0.044} \bar{g}_1) e \text{ fm} \right], \quad (4.5)$$

$$d_{\text{Yb}} = -2.10_{-0.0}^{+0.22} \cdot 10^{-4} \left[0.54_{-0.11}^{+0.13} d_n + 0.054_{-0.014}^{+0.016} d_p + \frac{g^{AmN}}{f_\pi} (0.01_{-0.0}^{+0.02} \bar{g}_0 + 0.02_{-0.027}^{+0.034} \bar{g}_1) e \text{ fm} \right], \quad (4.6)$$

$$d_{\text{Ra}} = -8.5_{-0.3}^{+0.25} \cdot 10^{-4} \left[0.63_{-0.12}^{+0.16} d_n + 0.14_{-0.03}^{+0.04} d_p + \frac{g^{AmN}}{f_\pi} (-0.2(6) \bar{g}_0 + 5(3) \bar{g}_1) e \text{ fm} + m_N^3 (-0.01(3) C_1 + 0.03(2) C_2) e \text{ fm} \right], \quad (4.7)$$

where we have neglected contributions from the electron EDM d_e and the electron–nucleon coupling C_S , to which diamagnetic atoms are less sensitive than paramagnetic systems (see the following subsection). Theoretical uncertainties are sizable, particularly for contributions from CP-odd nuclear interactions (i.e., \bar{g}_0 , \bar{g}_1 , C_1 , and C_2). The EDMs of these neutral atoms are screened by atomic electrons, so that the observable EDMs are proportional to the nuclear Schiff moments [88, 89]. This leads to a suppression of order 10^{-5} – 10^{-4} relative to nucleon EDMs. Nevertheless, as shown in Table 1, this suppression is compensated by the high experimental sensitivity achievable with heavy atoms, owing to large atom numbers, long spin-coherence times, and advanced comagnetometry techniques (see, e.g., [2]). Furthermore, systems with octupole-deformed nuclei, such as ^{225}Ra , can exhibit a strong enhancement of Schiff moments induced by CP-odd nuclear interactions [90–92]. Although EDM experiments for such systems are still at an early stage, they are expected to provide powerful probes of CP-odd nuclear interactions in the future, with projected sensitivities reaching the level of 10^{-28} e cm for d_{Ra} [93].

Given the current experimental bounds summarized in Table 1 and the theoretical expressions in Eqs. (4.4)–(4.7), the EDM of ^{199}Hg provides the most stringent constraints on d_p , \bar{g}_0 , and \bar{g}_1 at present. Assuming no cancellations among the contributions of d_p , d_n , \bar{g}_0 , and \bar{g}_1 to d_{Hg} , the experimental upper limit on d_{Hg} implies [94]

$$|d_p| < 2.0 \times 10^{-25} \text{ e cm}, \quad |\bar{g}_0| < 2.3 \times 10^{-12}, \quad |\bar{g}_1| < 1.1 \times 10^{-12}. \quad (4.8)$$

System i	Upper limit on $ d_i $ [e cm]
n	$2.2 \cdot 10^{-26}$ [95]
^{199}Hg	$7.4 \cdot 10^{-30}$ [94]
^{129}Xe	$1.4 \cdot 10^{-27}$ [96, 97]
^{171}Yb	$1.5 \cdot 10^{-26}$ [98]
^{225}Ra	$1.4 \cdot 10^{-23}$ [93]
HfF^+	$4.8 \cdot 10^{-30}$ [99]
ThO	$1.1 \cdot 10^{-29}$ [100]
YbF	$1.2 \cdot 10^{-27}$ [101]

Table 1: Experimental upper limits on the EDMs $|d_i|$ of system i are summarized. For polar molecules (HfF^+ , ThO , YbF), the quoted EDM corresponds to a quantity defined through the P -odd and T -odd frequency shift of spin precession, rather than the permanent molecular EDM arising from an asymmetric charge distribution within the molecule, which exists independently of fundamental CP-violating interactions. For a precise definition, see Sec. 4.2.

4.2 Paramagnetic systems

Paramagnetic systems contain at least one unpaired electron in atoms or molecules and are therefore sensitive to interactions involving electrons. In particular, polar molecules can be

highly sensitive to CP-violating (CPV) observables such as the electron EDM d_e and the electron–nucleon coupling C_S ¹⁰, because they can possess strong internal effective electric fields arising from their asymmetric molecular structure. In the following, we consider HfF^+ , ThO , and YbF .

Since polar molecules already have nonzero permanent EDMs associated with asymmetric charge distributions, which do not violate P and T symmetries, the P -odd and T -odd component induced by fundamental CPV interactions is conventionally characterized by the corresponding frequency shift of electron spin precession, which is directly measurable in EDM experiments. The P -odd and T -odd frequency shifts induced by d_e and C_S are summarized in Refs. [8, 23], based on Refs. [103–105] for HfF^+ , Refs. [106–109] for ThO , and Refs. [107, 110, 111] for YbF :

$$\omega_{\text{HfF}^+} = 3.49(14) \times 10^{28} d_e [\text{mrad/s}][e \text{ cm}]^{-1} + 3.20(13) \times 10^8 C_S [\text{mrad/s}], \quad (4.9)$$

$$\omega_{\text{ThO}} = -1.206(49) \times 10^{29} d_e [\text{mrad/s}][e \text{ cm}]^{-1} - 1.816(73) \times 10^9 C_S [\text{mrad/s}], \quad (4.10)$$

$$\omega_{\text{YbF}} = -1.96(15) \times 10^{28} d_e [\text{mrad/s}][e \text{ cm}]^{-1} - 1.76(20) \times 10^8 C_S [\text{mrad/s}], \quad (4.11)$$

with theoretical uncertainties typically below the 10% level. In these expressions, the coefficient multiplying d_e corresponds to the effective electric field E_{eff} intrinsic to the molecular structure, independent of any applied external electric field.¹¹ Following Ref. [8], one may define an effective EDM for a given molecule i as $d_i \equiv \omega_i/E_{\text{eff}}$; the corresponding experimental upper limits on $|d_i|$ are given in Table 1.

Paramagnetic atoms such as Tl and Cs are also sensitive to d_e and C_S , although their sensitivities are typically two to three orders of magnitude weaker than those of polar molecules, primarily due to the absence of strong internal effective electric fields in atoms (see, e.g., [32, 112]). On the other hand, such systems can provide sensitive probes of nuclear spin-dependent CPV electron–nucleon interactions of the form $C_P \bar{e} e \bar{N} i \gamma_5 N + C_T \bar{e} \sigma^{\mu\nu} e \bar{N} \sigma_{\mu\nu} i \gamma_5 N$ [8, 113]. In this work, however, we do not consider these contributions, as the corresponding nuclear spin-dependent interactions are negligible for the UV sources discussed in Sec. 2.

Currently, the most stringent constraints on d_e and C_S are obtained from the EDM measurement of HfF^+ , yielding [99]

$$|d_e| < 4.1 \times 10^{-30} e \text{ cm}, \quad |C_S| < 4.4 \times 10^{-10}, \quad (4.12)$$

at 90% CL, assuming no cancellation between the contributions of d_e and C_S to ω_{HfF^+} .

Paramagnetic systems can also probe hadronic IR CPV parameters (d_p , d_n , \bar{g}_0 , \bar{g}_1) through the induced coupling C_S^{IR} in Eq. (3.66), which arises from long-distance hadronic interactions. To estimate the relative sensitivity of polar molecules to these hadronic CPV

¹⁰Ref. [102] shows that polar molecules can also provide sensitive probes for CPV nucleon–nucleon long range interactions mediated by a new light particle whose mass is below about 10 keV which corresponds to the inter-atomic distance scale of polar molecules.

¹¹An external electric field is nevertheless required in experiments to polarize the molecule and align the internal effective field.

parameters, we parametrize the P -odd and T -odd frequency shift of a polar molecule X as

$$\frac{\omega_X}{0.01 \text{ mrad/s}} = \alpha_X \frac{d_e}{10^{-30} [e \text{ cm}]} + \beta_X \frac{C_S}{10^{-10}}, \quad (4.13)$$

where α_X and β_X are typically of $\mathcal{O}(1)$, except for ThO, for which $\alpha_{\text{ThO}} \sim \beta_{\text{ThO}} \sim \mathcal{O}(10)$. The normalization factors are chosen to be close to the current experimental limits in Eq. (4.12). Using Eq. (3.68), we obtain

$$\frac{C_S^{\text{IR}}}{10^{-10}} \simeq -0.55 \frac{\bar{g}_0}{10^{-10}} + 2.2 \frac{\bar{g}_1}{10^{-10}} + 3.4 \frac{d_p}{10^{-23} [e \text{ cm}]} - 3.5 \frac{d_n}{10^{-23} [e \text{ cm}]}. \quad (4.14)$$

The coefficients vary by less than 10% across the polar molecules considered in EDM experiments. Comparing with Eq. (4.8), one finds that the current sensitivity of polar molecules to hadronic IR CPV parameters is approximately two to three orders of magnitude weaker than that of diamagnetic atoms.

5 Identification of the UV sources with EDM data

We now investigate *the EDM inverse problem* based on the state-of-the-art computations summarized in Secs. 3 and 4. Our goal is to assess whether the six classes of UV CP-violating (CPV) sources in Eq. (2.5) can be distinguished using future EDM data, taking into account theoretical uncertainties. Among the sources in Eq. (2.5), the hadronic CPV sources $X_i^{\text{UV}} \in \{\bar{\theta}, w, \tilde{d}_q, d_q\}$ are most sensitively probed by light nuclei and diamagnetic atoms, as discussed in Sec. 4.1, whereas the (semi-)leptonic sources $X_i^{\text{UV}} \in \{d_e, \text{Im}(C_{eeDD})\}$ are best probed by polar molecules, as discussed in Sec. 4.2. We therefore analyze these two classes separately.

5.1 Hadronic sources

5.1.1 Single source

A simple and plausible working assumption is that CP violation is dominated by a single hadronic UV source among $X_i^{\text{UV}} \in \{\bar{\theta}, w, w^{\text{PQ}}, \tilde{d}_q, \tilde{d}_q^{\text{PQ}}, d_q\}$, where the superscript ‘‘PQ’’ denotes quantities in the presence of the PQ mechanism. Under this assumption, one can predict characteristic ratios of EDMs for light nuclei and diamagnetic atoms. From

Eqs. (4.2)–(4.7), we obtain

$$\frac{d_D}{d_n} = 0.94(1) \left(1 + \frac{d_p}{d_n} \right) + 1.05(12) \frac{e\bar{g}_1}{\Lambda_\chi d_n}, \quad (5.1)$$

$$\frac{d_{\text{He}}}{d_n} = 0.9 - 0.03(1) \frac{d_p}{d_n} + 0.64(6) \frac{e\bar{g}_0}{\Lambda_\chi d_n} + 0.82(12) \frac{e\bar{g}_1}{\Lambda_\chi d_n} - 0.18(9) \frac{ef_\pi^2 C_1}{d_n}, \quad (5.2)$$

$$\frac{d_{\text{Hg}}}{d_n} = \left(-2.7(17) - 0.35(24) \frac{d_p}{d_n} - 5(4) \frac{e\bar{g}_0}{\Lambda_\chi d_n} - 5(11) \frac{e\bar{g}_1}{\Lambda_\chi d_n} \right) \times 10^{-4}, \quad (5.3)$$

$$\frac{d_{\text{Xe}}}{d_n} = \left(2.4(5) + 0.51(11) \frac{d_p}{d_n} - 8(6) \frac{e\bar{g}_0}{\Lambda_\chi d_n} + 7(7) \frac{e\bar{g}_1}{\Lambda_\chi d_n} \right) \times 10^{-5}, \quad (5.4)$$

$$\frac{d_{\text{Yb}}}{d_n} = \left(-4(5) - 0.109(30) \frac{d_p}{d_n} - 3.1(16) \frac{e\bar{g}_0}{\Lambda_\chi d_n} - 4(5) \frac{e\bar{g}_1}{\Lambda_\chi d_n} \right) \times 10^{-4}, \quad (5.5)$$

$$\begin{aligned} \frac{d_{\text{Ra}}}{d_n} = & \left(-5.5(12) - 1.24(30) \frac{d_p}{d_n} \right) \times 10^{-4} + 0.01(4) \frac{e\bar{g}_0}{\Lambda_\chi d_n} - 0.33(20) \frac{e\bar{g}_1}{\Lambda_\chi d_n} \\ & + 0.004(13) \frac{ef_\pi^2 C_1}{d_n}, \end{aligned} \quad (5.6)$$

where $\Lambda_\chi = 4\pi f_\pi$. These expressions show that each of the ratios d_p/d_n , $e\bar{g}_0/(\Lambda_\chi d_n)$, $e\bar{g}_1/(\Lambda_\chi d_n)$, and $ef_\pi^2 C_1/d_n$ contributes comparably to the EDM ratios d_X/d_n ($X = D, \text{He}, \text{Hg}, \text{Xe}, \text{Yb}, \text{Ra}$), unless the corresponding contribution is negligibly small.

Table 2 summarizes the relative importance of these contributions for different dominant CPV sources, based on the discussion in Sec. 3. In particular, if CP violation is dominated by quark CEDMs (\tilde{d}_q or \tilde{d}_q^{PQ}), the ratios d_X/d_n are largely controlled by $e\bar{g}_1/(\Lambda_\chi d_n)$. In contrast, if CP violation is dominated by quark EDMs (d_q), the ratios are primarily determined by d_p/d_n .

Table 3 summarizes the predicted EDM ratios for different dominant sources of CP violation, under the assumption that a single class of operators dominates. In each case, the ratios depend on at most one parameter: $r(\Lambda)$ for the w -dominated scenario, d_u/d_d for the d_q -dominated scenario, and \tilde{d}_u/\tilde{d}_d for the \tilde{d}_q -dominated scenario. Therefore, in principle, measurements of two independent EDM ratios in Table 3 can be used to identify the underlying source of CP violation.

The predicted values are subject to sizable theoretical uncertainties, particularly for heavy atoms such as ^{199}Hg , ^{225}Ra , and ^{129}Xe , which can exceed 100% in some cases. By contrast, the uncertainties are relatively smaller, typically below 50%, for light nuclei such as p , D , and $^3\text{He}^{++}$. Nevertheless, measurements of EDM ratios can still provide valuable guidance on the nature of the underlying CPV source.

In Fig. 1, we illustrate the results of Table 3 for a representative scenario in order to provide a qualitative picture of the EDM ratios. For this plot, we assume $\Lambda = 10$ TeV for the gluon CEDM-dominated case, and that the down-quark (C)EDM dominates over the up-quark (C)EDM, as motivated in supersymmetric extensions of the SM or type-II two-Higgs-doublet models with large $\tan\beta \gg 1$.

We now highlight several notable features of the predicted EDM ratios in Table 3 and Fig. 1. The results indicate that the \tilde{d}_q -dominated scenario, with or without the PQ mechanism, can be clearly distinguished from the other scenarios by large ratios of

	$\bar{\theta}$	w	w^{PQ}
$\frac{d_p}{d_n}$	-1.5	-0.90(3)	-0.90(3)
$\frac{e\bar{g}_0}{\Lambda_\chi d_n}$	3.5(6)	$0.08(28)r(\Lambda) \pm \frac{m_u+m_d}{f_\pi}$	$0.7(5)r(\Lambda) \pm \frac{m_u+m_d}{f_\pi}$
$\frac{e\bar{g}_1}{\Lambda_\chi d_n}$	-0.8(5)	$-4.8(33)r(\Lambda) \pm 0.11(9)$	$-4.8(33)r(\Lambda) \pm 0.11(9)$
$\frac{ef_\pi^2 C_1}{d_n}$	-	$0.1^{+2.1}_{-0.6}$	$0.1^{+2.1}_{-0.6}$

	d_q	\tilde{d}_q	\tilde{d}_q^{PQ}
$\frac{d_p}{d_n}$	$\frac{4d_u - d_d}{d_u - 4d_d}$	$\frac{0.81(6)\tilde{d}_u - 1.51(4)\tilde{d}_d}{0.64(4)\tilde{d}_u - 0.18(4)\tilde{d}_d}$	$\frac{8\tilde{d}_u + \tilde{d}_d}{2\tilde{d}_u + 4\tilde{d}_d}$
$\frac{e\bar{g}_0}{\Lambda_\chi d_n}$	-	$\frac{4(11)\tilde{d}_u + 2(10)\tilde{d}_d}{4.4(8)\tilde{d}_u - 1.2(11)\tilde{d}_d}$	$\frac{5.6(22)(\tilde{d}_u + \tilde{d}_d)}{\tilde{d}_u + 2\tilde{d}_d}$
$\frac{e\bar{g}_1}{\Lambda_\chi d_n}$	-	$\frac{-483(165)(\tilde{d}_u - \tilde{d}_d)}{4.4(8)\tilde{d}_u - 1.2(11)\tilde{d}_d}$	$\frac{99(37)(\tilde{d}_u - \tilde{d}_d)}{\tilde{d}_u + 2\tilde{d}_d}$
$\frac{ef_\pi^2 C_1}{d_n}$	-	-	-

Table 2: Ratios of IR CPV parameters to the neutron EDM arising from a single dominant UV CPV operator. For d_p/d_n , the ratios have to be understood to have at least 10% error from higher-order contributions in the OPE of the QCD sum rules for nucleon EDMs.

$\mathcal{O}(10^2)$ – $\mathcal{O}(10^3)$, driven by the sizable CP-odd pion–nucleon coupling \bar{g}_1 . By contrast, if the measured ratios are of $\mathcal{O}(1)$, this would suggest that the dominant CPV source is $\bar{\theta}$, w , or d_q .

For the d_q -dominated scenario, the predicted ratios exhibit relatively small theoretical uncertainties, enabling a clear experimental identification of the source. In contrast, it may be difficult to distinguish the $\bar{\theta}$ -dominated scenario from the w -dominated scenario given the current theoretical uncertainties. In this case, additional information such as relative sign differences among certain EDM ratios (e.g., d_D/d_n and d_{He}/d_n) may be required.

5.1.2 Multiple sources

The EDM ratios can deviate significantly from those in Table 3 if multiple CPV operators contribute comparably to the nuclear EDMs. In such cases, one must solve the corresponding linear system to determine the underlying CPV sources. Since the contribution of $C_1(w)$ is relatively small, we neglect it as an approximation. The remaining four IR CPV parameters, d_n , d_p , \bar{g}_0 , and \bar{g}_1 , can in principle be determined from four independent

	$\bar{\theta}$	w, w^{PQ}	d_q	\tilde{d}_q	\tilde{d}_q^{PQ}
$\frac{d_p}{d_n}$	-1.5	-0.90(3)	$-\frac{4d_u-d_d}{d_u-4d_d}$	$\frac{0.81(6)\tilde{d}_u-1.51(4)\tilde{d}_d}{0.64(4)\tilde{d}_u-0.18(4)\tilde{d}_d}$	$\frac{8\tilde{d}_u+\tilde{d}_d}{2\tilde{d}_u+4\tilde{d}_d}$
$\frac{d_D}{d_n}$	-1.3(5)	$-5.1(35)r(\Lambda) + 0.09(21)$	$-\frac{2.82(3)(d_u+d_d)}{d_u-4d_d}$	$\frac{-505(183)(\tilde{d}_u-\tilde{d}_d)}{4.4(8)\tilde{d}_u-1.2(11)\tilde{d}_d}$	$\frac{105(41)(\tilde{d}_u-\tilde{d}_d)}{\tilde{d}_u+2\tilde{d}_d}$
$\frac{d_{\text{He}}}{d_n}$	2.5(6)	$-3.9(28)r(\Lambda) + 0.77(31)$	$0.9 + 0.03(1)\frac{4d_u-d_d}{d_u-4d_d}$	$\frac{-396(147)(\tilde{d}_u-\tilde{d}_d)}{4.4(8)\tilde{d}_u-1.2(11)\tilde{d}_d}$	$\frac{81(32)(\tilde{d}_u-\tilde{d}_d)}{\tilde{d}_u+2\tilde{d}_d}$
$10^4 \frac{d_{\text{Hg}}}{d_n}$	-15(17)	$25(53)r(\Lambda) - 2.4(20)$	$-\frac{1.3(19)d_u+11(7)d_d}{d_u-4d_d}$	$\frac{3(5)\times 10^3(\tilde{d}_u-\tilde{d}_d)}{4.4(8)\tilde{d}_u-1.2(11)\tilde{d}_d}$	$-\frac{0.5(11)\times 10^3(\tilde{d}_u-\tilde{d}_d)}{\tilde{d}_u+2\tilde{d}_d}$
$10^5 \frac{d_{\text{Xe}}}{d_n}$	31(24)	$-36(40)r(\Lambda) + 1.9(17)$	$\frac{0.3(7)d_u-8.9(21)d_d}{d_u-4d_d}$	$\frac{-3.6(34)\times 10^3(\tilde{d}_u-\tilde{d}_d)}{4.4(8)\tilde{d}_u-1.2(11)\tilde{d}_d}$	$\frac{0.74(71)\times 10^3(\tilde{d}_u-\tilde{d}_d)}{\tilde{d}_u+2\tilde{d}_d}$
$10^4 \frac{d_{\text{Yb}}}{d_n}$	-9(7)	$17(26)r(\Lambda) - 1.0(8)$	$-\frac{0.66(27)d_u+4.3(10)d_d}{d_u-4d_d}$	$\frac{1.7(24)\times 10^3(\tilde{d}_u-\tilde{d}_d)}{4.4(8)\tilde{d}_u-1.2(11)\tilde{d}_d}$	$-\frac{0.36(49)\times 10^3(\tilde{d}_u-\tilde{d}_d)}{\tilde{d}_u+2\tilde{d}_d}$
$\frac{d_{\text{Ra}}}{d_n}$	0.31(27)	$1.6(14)r(\Lambda) + 0.00(7)$	$-\frac{0.6(17)d_u+21(5)d_d}{d_u-4d_d} \cdot 10^{-4}$	$\frac{160(110)(\tilde{d}_u-\tilde{d}_d)}{4.4(8)\tilde{d}_u-1.2(11)\tilde{d}_d}$	$-\frac{33(23)(\tilde{d}_u-\tilde{d}_d)}{\tilde{d}_u+2\tilde{d}_d}$

Table 3: Predicted nuclear and atomic EDMs, normalized to the neutron EDM, for scenarios with a single dominant UV CPV operator. For d_p/d_n and d_D/d_n , the ratios have to be understood to have at least 10% error from higher-order contributions in the OPE of the QCD sum rules for nucleon EDMs.

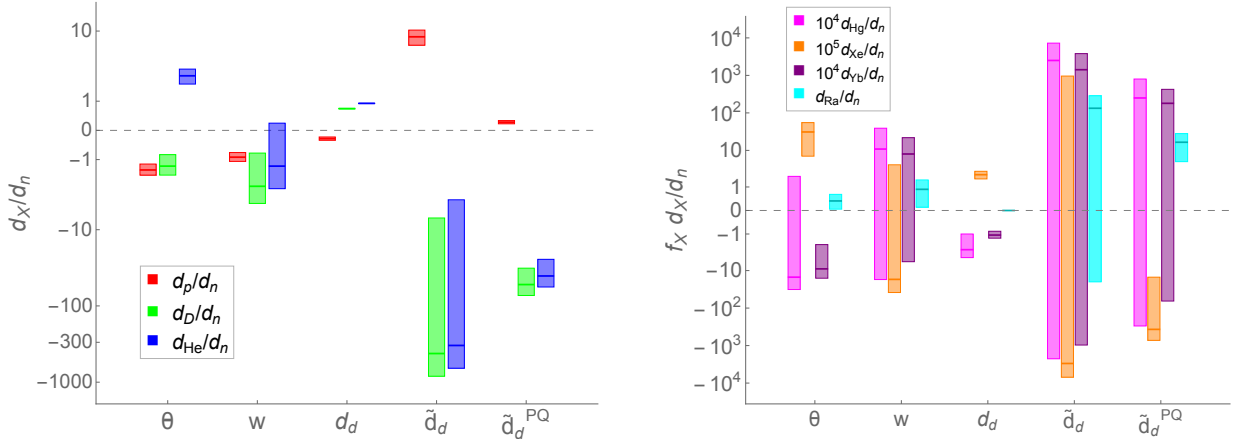


Figure 1: Illustration of Table 3 for a specific scenario with $\Lambda = 10$ TeV in the gluon CEDM-dominated case and down-quark (C)EDM dominance over the up-quark (C)EDM. In the right panel, $f_X = 10^4$ ($X = \text{Hg}, \text{Xe}$), 10^5 ($X = \text{Yb}$), and 1 ($X = \text{Ra}$) denote the normalization factors accounting for Schiff screening and octupole enhancement.

EDM measurements.

Given the theoretical uncertainties in Eqs. (4.2)–(4.7), EDM data from light nuclei (n , p , D , ${}^3\text{He}^{++}$) provide the most precise determination. In particular, inverting Eqs. (4.2) and (4.3) yields

$$\begin{pmatrix} d_n [\text{GeV}/e] \\ d_p [\text{GeV}/e] \\ \bar{g}_0 \\ \bar{g}_1 \end{pmatrix} = \mathcal{M}_{\text{IR}} \begin{pmatrix} d_n \\ d_p \\ d_D \\ d_{\text{He}} \end{pmatrix} [\text{GeV}/e], \quad (5.7)$$

where

$$\mathcal{M}_{\text{IR}} = \begin{pmatrix} 1 & 0 & 0 & 0 \\ 0 & 1 & 0 & 0 \\ -0.30(26) & 1.37(27) & -1.40(28) & 1.80(33) \\ -1.03(18) & -1.03(18) & 1.10(19) & 0 \end{pmatrix}. \quad (5.8)$$

This matrix determines the IR CPV parameters from the EDM data.

By contrast, the IR CPV parameters are poorly constrained by EDMs of heavy diamagnetic atoms due to large theoretical uncertainties. For example, using ${}^{199}\text{Hg}$, ${}^{129}\text{Xe}$, ${}^{225}\text{Ra}$, together with the neutron EDM, one finds

$$\begin{pmatrix} d_n [\text{GeV}/e] \\ d_p [\text{GeV}/e] \\ \bar{g}_0 \\ \bar{g}_1 \end{pmatrix} = \mathcal{M}_{\text{IR}} \begin{pmatrix} d_n \\ d_{\text{Hg}} \\ d_{\text{Xe}} \\ d_{\text{Ra}} \end{pmatrix} [\text{GeV}/e], \quad (5.9)$$

with

$$\mathcal{M}_{\text{IR}} = \begin{pmatrix} 1 & 0 & 0 & 0 \\ -6(7) & -1.4(20) \times 10^4 & 1.0(13) \times 10^5 & 45(69) \\ -0.13(34) & -1.1(12) \times 10^3 & -8(10) \times 10^3 & 0(4) \\ 0.00(4) & -39(142) & -0.4(10) \times 10^3 & -4(4) \end{pmatrix}, \quad (5.10)$$

where most entries carry theoretical uncertainties exceeding 100%. Therefore, precise EDM measurements of light nuclei are essential for disentangling CPV sources when multiple contributions are present, unless theoretical calculations for heavy diamagnetic atoms are significantly improved.

After determining $(d_n, d_p, \bar{g}_0, \bar{g}_1)$, one can at most disentangle four independent UV CPV sources among the six possible sources $(\bar{\theta}, w, d_u, d_d, \tilde{d}_u, \tilde{d}_d)$, either with or without the PQ mechanism. Since the presence of quark CEDMs is signaled by a large ratio $e\bar{g}_1/(\Lambda_\chi d_n) \gg 1$, it is useful to classify possible scenarios according to the size of this ratio.

- $e\bar{g}_1/(\Lambda_\chi d_n) \gg 1$

A large value of this ratio indicates that quark CEDMs are likely to be involved in the CPV source, unless there is a fine-tuned cancellation among different contributions. In many UV scenarios that generate quark CEDMs, such as supersymmetric

extensions of the SM or type-II 2HDMs, quark EDMs are typically of comparable magnitude, since both arise from loops involving colored particles carrying electric charge [2, 28]. By contrast, the QCD θ term and the gluon CEDM usually arise from distinct physical origins. It is therefore well motivated to consider scenarios in which quark CEDMs and quark EDMs contribute simultaneously to nuclear EDMs:

$$\begin{pmatrix} \tilde{d}_u \\ \tilde{d}_d \\ d_u \\ d_d \end{pmatrix} [\text{GeV}] = \mathcal{M}_{\text{UV}}^{(\text{PQ})} \begin{pmatrix} d_n [\text{GeV}/e] \\ d_p [\text{GeV}/e] \\ \bar{g}_0 \\ \bar{g}_1 \end{pmatrix}, \quad (5.11)$$

where $\mathcal{M}_{\text{UV}}^{(\text{PQ})}$ determines the UV parameters from the IR ones, and depends on whether the PQ mechanism is present. Without the PQ mechanism, we obtain

$$\mathcal{M}_{\text{UV}} = \begin{pmatrix} 0 & 0 & -2(9) & 0.00(6) \\ 0 & 0 & -2(9) & -0.02(10) \\ 0.3(22) & 1(9) & 0.7(33) & 0.02(12) \\ 1(9) & 0.3(22) & -0.3(17) & 0.01(6) \end{pmatrix}, \quad (5.12)$$

whose precision is rather poor, mainly due to the large theoretical uncertainty in $\bar{g}_0(\tilde{d}_q)$ in Eq. (3.38). In contrast, in the presence of the PQ mechanism, we find

$$\mathcal{M}_{\text{UV}}^{\text{PQ}} = \begin{pmatrix} 0 & 0 & 0.23(8) & 0.013(4) \\ 0 & 0 & 0.23(8) & -0.013(4) \\ 0.327(27) & 1.31(11) & 0.38(14) & 0.022(8) \\ 1.31(11) & 0.327(27) & -0.19(7) & 0.011(4) \end{pmatrix}, \quad (5.13)$$

which exhibits significantly improved precision.

- $e\bar{g}_1/(\Lambda_\chi d_n) \sim \mathcal{O}(1)$

In this case, CPV sources other than quark CEDMs (i.e. $\bar{\theta}$, w , d_u , and d_d) may contribute comparably to the nuclear EDMs. One can then write

$$\begin{pmatrix} \bar{\theta} \\ w [\text{GeV}]^2 \\ d_u [\text{GeV}] \\ d_d [\text{GeV}] \end{pmatrix} = \mathcal{M}_{\text{UV}}(\Lambda) \begin{pmatrix} d_n [\text{GeV}/e] \\ d_p [\text{GeV}/e] \\ \bar{g}_0 \\ \bar{g}_1 \end{pmatrix}, \quad (5.14)$$

where $\mathcal{M}_{\text{UV}}(\Lambda)$ depends on the scale Λ at which the Weinberg operator is generated, through the RG factor $r(\Lambda)$ in Eq. (2.23). For $\Lambda \gtrsim 1$ TeV, we find

$$\mathcal{M}_{\text{UV}}(\Lambda) = \begin{pmatrix} 0 & 0 & 66(36) & A \pm 5.4(24) r^{-1} \\ 0 & 0 & -2.0(17) r^{-1} & -9(4) r^{-1} \\ 0.33(18) & 1.3(7) & 0.42(23) - 0.034(35) r^{-1} & -0.16(12) r^{-1} + 0.06(4) \\ 1.3(7) & 0.33(18) & -0.21(12) + 0.04(4) r^{-1} & 0.19(14) r^{-1} - 0.032(18) \end{pmatrix}, \quad (5.15)$$

where the coefficient A depends on the presence of the PQ mechanism: $A = -1.0(29)$ without PQ and $A = 10(6)$ with PQ.

5.2 (Semi-)leptonic sources

Among the UV CPV sources in Eqs. (2.2)–(2.4), those involving electrons, namely the electron EDM and the CPV electron-down quark coupling, can be probed with high sensitivity by paramagnetic systems, in particular polar molecules, as discussed in Sec. 4.2.

	d_e	C_S
$\frac{\omega_{\text{ThO}}}{\omega_{\text{HfF}^+}}$	-3.46(20)	-5.68(32)
$\frac{\omega_{\text{YbF}}}{\omega_{\text{HfF}^+}}$	-0.56(5)	-0.55(7)

Table 4: Predicted EDMs of polar molecules, normalized to that of HfF^+ , for scenarios in which either d_e or C_S dominates.

In Table 4, we present the predicted ratios of the P -odd and T -odd frequency shifts for the polar molecules HfF^+ , ThO , and YbF , assuming that CP violation is dominated by either d_e or C_S . The ratios are obtained from Eqs. (4.9)–(4.11). They show that d_e can be clearly distinguished from C_S using the EDM data of ThO together with that of another polar molecule as also discussed in [23], since the theoretical uncertainties are typically below $\sim 10\%$ level.

If the dominant CPV source is C_S , the relevant UV sources among those in Eqs. (2.2)–(2.4) are the electron-down quark CPV coupling and hadronic operators that induce C_S via long-distance electromagnetic interactions, as discussed in Sec. 3.4. These two classes can be discriminated by EDM measurements of light nuclei and diamagnetic atoms, since hadronic operators generically induce sizable EDMs in those systems, whereas the electron-down quark CPV coupling does not.

If C_S originates from hadronic operators, one expects observable signals in light nuclei or diamagnetic atoms with magnitudes given by either $d_{n,p} \sim 10^{-13} e \text{ cm} \times C_S$ or $\bar{g}_{0,1} \sim C_S$, as inferred from Eq. (3.68).

If the measured ratios deviate from the predictions in Table 4, this indicates that both d_e and C_S contribute comparably to the EDMs of polar molecules.¹² In that case, one must solve the linear system in Eqs. (4.9)–(4.11) to extract d_e and C_S from the data. For example, inverting Eqs. (4.9) and (4.10) yields

$$\begin{pmatrix} d_e [e \text{ cm}]^{-1} \\ C_S \end{pmatrix} = \begin{pmatrix} 7.3(13) \times 10^{-29} & 1.29(23) \times 10^{-29} \\ -4.9(9) \times 10^{-9} & -1.41(25) \times 10^{-9} \end{pmatrix} \begin{pmatrix} \omega_{\text{HfF}^+} \\ \omega_{\text{ThO}} \end{pmatrix} [\text{mrad/s}]^{-1}, \quad (5.16)$$

where the theoretical uncertainties are below 20%. Thus, measurements of two different polar molecules allow a determination of both d_e and C_S .

¹²According to Ref. [102], there is another possibility that the ratios are due to CPV nucleon-nucleon long range interactions mediated by a new particle lighter than 10 keV.

6 Conclusions

In this work, we investigate the feasibility of inferring ultraviolet (UV) sources of CP violation (CPV) from precision measurements of electric dipole moments (EDMs) of light nuclei, atoms, and molecules. We first identify six important classes of CPV operators at the QCD scale that arise in the Standard Model (SM) and in well-motivated beyond-the-SM (BSM) scenarios. These operators, listed in Eq. (2.5), are the QCD θ term, the gluon chromo-electric dipole moment (CEDM), often referred to as the Weinberg three-gluon operator, quark CEDMs, quark EDMs, the electron EDM, and CP-odd electron–down-quark interactions.

Among these six classes, the four hadronic operators that do not involve electrons can be probed with high sensitivity through EDM measurements of light nuclei and diamagnetic atoms. If the observed EDMs are dominated by a single operator class, the resulting EDM ratios depend on only one parameter. Consequently, precision measurements of at least three different nuclei or atoms, providing two independent EDM ratios, can in principle identify the dominant hadronic UV CPV source. Given current theoretical uncertainties, we find that EDM measurements of three light nuclei, such as the neutron (n), proton (p), and deuteron (D), are particularly powerful for discriminating among the four classes of hadronic operators. This observation strongly motivates storage-ring experiments that can directly measure the EDMs of charged light nuclei. While EDMs of heavy diamagnetic atoms such as ^{199}Hg , ^{129}Xe , and ^{171}Yb may provide suggestive information, they are not sufficient to draw definitive conclusions. Octupole-deformed systems such as ^{225}Ra offer improved sensitivity compared with ordinary heavy atoms, but still provide less discriminatory power than light nuclei.

If the dominant hadronic UV CPV source is found to be either the QCD θ term or quark CEDMs, as indicated by the corresponding EDM ratios in Table 3, this would also shed light on the origin of a nonzero QCD axion vacuum expectation value (VEV). Assuming that the strong CP problem is solved by the QCD axion, a $\bar{\theta}$ -dominated scenario would suggest that the axion VEV arises primarily from PQ-breaking effects other than the QCD anomaly, such as quantum-gravitational effects. In contrast, in quark-CEDM-dominated scenarios, EDM ratios can first be used to determine the presence or absence of the Peccei–Quinn (PQ) mechanism. If the observed ratios are consistent with the predictions for quark CEDMs in the presence of PQ symmetry, this would indicate that the QCD axion VEV is predominantly induced by quark CEDMs in conjunction with the standard PQ breaking by the QCD anomaly.

The remaining two classes of UV CPV operators involving electrons, namely the electron EDM and CP-odd electron–down-quark interactions, can be independently tested through EDM measurements of paramagnetic systems, in particular polar molecules. Electron EDMs can be clearly distinguished from CP-odd electron–nucleon interactions by observing nonvanishing EDMs in ThO and at least one additional polar molecule, provided the experimental uncertainties are below approximately 10%. If the dominant CPV source involves a nonzero CP-odd electron–nucleon coupling, its UV origin may be either the electron–down-quark interaction or long-distance hadronic effects induced by hadronic

UV CPV sources. These two possibilities can be discriminated by the presence of correspondingly large EDMs in light nuclei or diamagnetic atoms, characterized by either $d_{n,p} \sim 10^{-13} e \text{ cm} \times C_S$ or $\bar{g}_{0,1} \sim C_S$.

It should be emphasized that many of the currently available theoretical calculations used to connect CPV operators at the QCD scale to experimentally measured EDMs are subject to intrinsic uncertainties that cannot be reliably quantified with the present level of theoretical understanding of the relevant QCD, nuclear, and atomic physics effects. Our results should therefore be interpreted with these uncertainties in mind. Our primary goal is to assess how far one can proceed using currently available theoretical inputs, while also motivating future theoretical efforts toward a more quantitative understanding of the matching relations relevant for EDMs.

In conclusion, future high-precision EDM measurements have the potential to provide profound insights into the underlying UV physics, allowing, in principle, the identification of SM contributions, key classes of BSM scenarios, the PQ mechanism, and the origin of PQ symmetry breaking. Further efforts to reduce theoretical uncertainties, particularly through lattice QCD calculations and complementary theoretical tools, are therefore strongly motivated.

Acknowledgments

This work was supported by the Institute for Basic Science (IBS) under project code IBS-R018-D1. We thank Nodoka Yamanaka and Tae-Sun Park for helpful discussions.

A Naïve Dimensional Analysis for hadronic CP-odd quantities

In this appendix, we estimate the hadronic IR CPV parameters $X_i^{\text{IR}} \in \{d_n, d_p, \bar{g}_0, \bar{g}_1, C_1, C_2\}$ induced by the non-leptonic UV CPV parameters $X_i^{\text{UV}} \in \{\bar{\theta}, w, \tilde{d}_q, d_q\}$ ($q = u, d, s$), using naive dimensional analysis (NDA), in order to compare with the estimates presented in Sec. 3.

Applying the NDA rules of Refs. [72, 114, 115], and taking into account chiral and isospin symmetries, we obtain

$$d_{n,p} \sim e \frac{m_*}{\Lambda_\chi^2} \bar{\theta} + e \tilde{d}_{u,d,s} + d_{u,d,s} + e f_\pi w, \quad (\text{A.1})$$

$$\bar{g}_0 \sim \frac{m_*}{f_\pi} \bar{\theta} + 4\pi \Lambda_\chi \tilde{d}_{u,d} + (m_u + m_d) \Lambda_\chi w, \quad (\text{A.2})$$

$$\bar{g}_1 \sim \frac{(m_u - m_d)}{m_s} \frac{m_*}{f_\pi} \bar{\theta} + 4\pi \Lambda_\chi (\tilde{d}_u - \tilde{d}_d) + (m_u - m_d) \Lambda_\chi w, \quad (\text{A.3})$$

$$C_{1,2} \sim \frac{m_*}{f_\pi^2 \Lambda_\chi^2} \bar{\theta} + \frac{1}{f_\pi^2} (\tilde{d}_u + \tilde{d}_d) + \frac{1}{f_\pi} w, \quad (\text{A.4})$$

evaluated at the matching scale $\mu_{\text{NDA}} = 225 \text{ MeV}$, defined by $\alpha_s(\mu_{\text{NDA}})/(4\pi) \simeq 1/6$, where the one-loop QCD beta function becomes comparable to the two-loop contribution [72]. Here $m_* \equiv \left(\sum_{q=u,d,s} m_q^{-1}\right)^{-1} \simeq m_u m_d / (m_u + m_d)$ and $\Lambda_\chi = 4\pi f_\pi$. These expressions should be regarded as order-of-magnitude estimates with undetermined overall signs.

Several remarks are in order. First, for the definition of the quark CEDMs \tilde{d}_q , we adopt the convention of Eq. (2.3), in which the QCD coupling $g_s(\mu_{\text{NDA}}) \sim 4\pi$ is absorbed into the operator. Second, the quark CEDM contribution to \bar{g}_0 is not necessarily proportional to $\text{Tr}(\tilde{d}_q) = \tilde{d}_u + \tilde{d}_d$, since there exists an additional isospin-invariant contribution proportional to $\text{Tr}(M_q^{-1}\tilde{d}_q) = \sum_q \tilde{d}_q/m_q$, arising from the effective CP-odd quark mass induced by \tilde{d}_q [68]. NDA suggests that these two contributions can be comparable. However, Ref. [68] shows, using QCD sum rules, that the contribution proportional to $\text{Tr}(M_q^{-1}\tilde{d}_q)$ is exactly canceled by the shift of the QCD axion VEV in the presence of the Peccei–Quinn (PQ) mechanism.

On the other hand, NDA indicates that, for \bar{g}_1 , the contribution proportional to $\text{Tr}(M_q^{-1}\tilde{d}_q)$ is negligible compared to that proportional to $\text{Tr}(\tilde{d}_q\tau_3)$. Consequently, \bar{g}_1 is approximately proportional to $\tilde{d}_u - \tilde{d}_d$. Finally, in estimating \bar{g}_1 from $\bar{\theta}$, we use the fact from chiral perturbation theory that the leading contribution arises from $\eta-\pi^0$ mixing combined with the $\eta\bar{N}N$ coupling.

The expressions in Eqs. (A.1)–(A.4) cannot be directly compared with the results in Sec. 3, since the matching scales differ. While NDA uses $\mu_{\text{NDA}} = 225$ MeV, most estimates in Sec. 3 are given at $\mu = 1$ GeV. To translate between these scales, we use the renormalization group (RG) relations

$$d_q(1 \text{ GeV})/d_q(\mu_{\text{NDA}}) \sim 1, \quad (\text{A.5})$$

$$\tilde{d}_q(1 \text{ GeV})/\tilde{d}_q(\mu_{\text{NDA}}) \sim 1, \quad (\text{A.6})$$

$$m_q(1 \text{ GeV})/m_q(\mu_{\text{NDA}}) \sim \frac{1}{2}, \quad (\text{A.7})$$

$$g_s(1 \text{ GeV})/g_s(\mu_{\text{NDA}}) \sim \frac{1}{2}, \quad (\text{A.8})$$

$$w(1 \text{ GeV})/w(\mu_{\text{NDA}}) \sim 2, \quad (\text{A.9})$$

as obtained from the RG equations in Sec. 2.2.

Using these relations, we find the NDA estimates at $\mu = 1$ GeV:

$$d_{n,p} \sim 3 \times 10^{-3} e \text{ GeV}^{-1} \bar{\theta} + e \tilde{d}_{u,d,s} + d_{u,d,s} + 0.04 e \text{ GeV} w, \quad (\text{A.10})$$

$$\bar{g}_0 \sim 3.8 \times 10^{-2} \bar{\theta} + 13 \text{ GeV} \tilde{d}_{u,d} + 7 \times 10^{-3} \text{ GeV}^2 w, \quad (\text{A.11})$$

$$\bar{g}_1 \sim 1.0 \times 10^{-3} \bar{\theta} + 13 \text{ GeV}(\tilde{d}_u - \tilde{d}_d) + 2.5 \times 10^{-3} \text{ GeV}^2 w, \quad (\text{A.12})$$

$$C_{1,2} \sim 0.3 \text{ GeV}^{-3} \bar{\theta} + 120 \text{ GeV}^{-2}(\tilde{d}_u + \tilde{d}_d) + 10 \text{ GeV}^{-1} w, \quad (\text{A.13})$$

where \tilde{d}_q , d_q , and w are evaluated at $\mu = 1$ GeV.

Overall, the NDA estimates are in agreement with the dedicated computations discussed in Sec. 3 up to factors of $O(1)$. The main exceptions are $\bar{g}_0(\tilde{d}_q)$ and $\bar{g}_0^{\text{PQ}}(\tilde{d}_q)$ in Eqs. (3.37) and (3.38), which are smaller than the NDA estimates by factors of ~ 10 and ~ 5 , respectively. The factor ~ 10 suppression in $\bar{g}_0(\tilde{d}_q)$ can be partially attributed to cancellations between the contributions proportional to $\text{Tr}(\tilde{d}_q)$ and $\delta m_N \text{Tr}(M_q^{-1}\tilde{d}_q)$.

References

- [1] M. Trodden, “Electroweak baryogenesis,” *Rev. Mod. Phys.* **71** (1999) 1463–1500, [arXiv:hep-ph/9803479](https://arxiv.org/abs/hep-ph/9803479).

- [2] T. Chupp, P. Fierlinger, M. Ramsey-Musolf, and J. Singh, “Electric dipole moments of atoms, molecules, nuclei, and particles,” *Rev. Mod. Phys.* **91** no. 1, (2019) 015001, [arXiv:1710.02504 \[physics.atom-ph\]](#).
- [3] Y. Cai, J. Herrero-García, M. A. Schmidt, A. Vicente, and R. R. Volkas, “From the trees to the forest: a review of radiative neutrino mass models,” *Front. in Phys.* **5** (2017) 63, [arXiv:1706.08524 \[hep-ph\]](#).
- [4] S. Okawa, M. Pospelov, and A. Ritz, “Electric Dipole Moments From Dark Sectors,” *Phys. Rev. D* **100** no. 7, (2019) 075017, [arXiv:1905.05219 \[hep-ph\]](#).
- [5] M. Pospelov and A. Ritz, “Electric Dipole Moments and New Physics,” [arXiv:2509.23531 \[hep-ph\]](#).
- [6] T. Chupp and M. Ramsey-Musolf, “Electric Dipole Moments: A Global Analysis,” *Phys. Rev. C* **91** no. 3, (2015) 035502, [arXiv:1407.1064 \[hep-ph\]](#).
- [7] K. Gaul and R. Berger, “Global analysis of \mathcal{CP} -violation in atoms, molecules and role of medium-heavy systems,” *JHEP* **08** (2024) 100, [arXiv:2312.08858 \[hep-ph\]](#).
- [8] S. Degenkolb, N. Elmer, T. Modak, M. Mühlleitner, and T. Plehn, “A Global View of the EDM Landscape,” *SciPost Phys.* **20** (2026) 151, [arXiv:2403.02052 \[hep-ph\]](#).
- [9] J. de Vries, R. Higa, C. P. Liu, E. Mereghetti, I. Stetcu, R. G. E. Timmermans, and U. van Kolck, “Electric Dipole Moments of Light Nuclei From Chiral Effective Field Theory,” *Phys. Rev. C* **84** (2011) 065501, [arXiv:1109.3604 \[hep-ph\]](#).
- [10] W. Dekens, J. de Vries, J. Bsaisou, W. Bernreuther, C. Hanhart, U.-G. Meißner, A. Nogga, and A. Wirzba, “Unraveling models of CP violation through electric dipole moments of light nuclei,” *JHEP* **07** (2014) 069, [arXiv:1404.6082 \[hep-ph\]](#).
- [11] J. de Vries, P. Draper, K. Fuyuto, J. Kozaczuk, and D. Sutherland, “Indirect Signs of the Peccei-Quinn Mechanism,” *Phys. Rev. D* **99** no. 1, (2019) 015042, [arXiv:1809.10143 \[hep-ph\]](#).
- [12] J. de Vries, P. Draper, K. Fuyuto, J. Kozaczuk, and B. Lillard, “Uncovering an axion mechanism with the EDM portfolio,” *Phys. Rev. D* **104** no. 5, (2021) 055039, [arXiv:2107.04046 \[hep-ph\]](#).
- [13] K. Choi, S. H. Im, and K. Jodłowski, “Exploring CP violation beyond the Standard Model and the PQ quality with electric dipole moments,” *JHEP* **04** (2024) 007, [arXiv:2308.01090 \[hep-ph\]](#).
- [14] R. D. Peccei and H. R. Quinn, “CP Conservation in the Presence of Instantons,” *Phys. Rev. Lett.* **38** (1977) 1440–1443.
- [15] S. Weinberg, “A New Light Boson?,” *Phys. Rev. Lett.* **40** (1978) 223–226.
- [16] F. Wilczek, “Problem of Strong P and T Invariance in the Presence of Instantons,” *Phys. Rev. Lett.* **40** (1978) 279–282.
- [17] A. Y. Morozov, “MATRIX OF MIXING OF SCALAR AND VECTOR MESONS OF DIMENSION $D \leq 8$ IN QCD. (IN RUSSIAN),” *Sov. J. Nucl. Phys.* **40** (1984) 505.
- [18] D. Chang, K. Choi, and W.-Y. Keung, “Induced Θ Contribution to the Neutron Electric Dipole Moment,” *Phys. Rev. D* **44** (1991) 2196–2199.
- [19] A. E. Nelson, “Naturally Weak CP Violation,” *Phys. Lett. B* **136** (1984) 387–391.

- [20] S. M. Barr, “Solving the Strong CP Problem Without the Peccei-Quinn Symmetry,” *Phys. Rev. Lett.* **53** (1984) 329.
- [21] M. Dine, “The Problem of Axion Quality: A Low Energy Effective Action Perspective,” [arXiv:2207.01068 \[hep-ph\]](#).
- [22] **pEDM** Collaboration, J. Alexander *et al.*, “Status of the Proton EDM Experiment (pEDM),” [arXiv:2504.12797 \[hep-ex\]](#).
- [23] T. Fleig and M. Jung, “Model-independent determinations of the electron EDM and the role of diamagnetic atoms,” *JHEP* **07** (2018) 012, [arXiv:1802.02171 \[hep-ph\]](#).
- [24] B. Grzadkowski, M. Iskrzynski, M. Misiak, and J. Rosiek, “Dimension-Six Terms in the Standard Model Lagrangian,” *JHEP* **10** (2010) 085, [arXiv:1008.4884 \[hep-ph\]](#).
- [25] T. Ibrahim and P. Nath, “The Neutron and the electron electric dipole moment in N=1 supergravity unification,” *Phys. Rev. D* **57** (1998) 478–488, [arXiv:hep-ph/9708456](#). [Erratum: *Phys.Rev.D* 58, 019901 (1998), Erratum: *Phys.Rev.D* 60, 079903 (1999), Erratum: *Phys.Rev.D* 60, 119901 (1999)].
- [26] D. Chang, W.-Y. Keung, and A. Pilaftsis, “New two loop contribution to electric dipole moment in supersymmetric theories,” *Phys. Rev. Lett.* **82** (1999) 900–903, [arXiv:hep-ph/9811202](#). [Erratum: *Phys.Rev.Lett.* 83, 3972 (1999)].
- [27] S. Abel, S. Khalil, and O. Lebedev, “EDM constraints in supersymmetric theories,” *Nucl. Phys. B* **606** (2001) 151–182, [arXiv:hep-ph/0103320](#).
- [28] M. Jung and A. Pich, “Electric Dipole Moments in Two-Higgs-Doublet Models,” *JHEP* **04** (2014) 076, [arXiv:1308.6283 \[hep-ph\]](#).
- [29] R. Barbieri, A. Pomarol, R. Rattazzi, and A. Strumia, “Electroweak symmetry breaking after LEP-1 and LEP-2,” *Nucl. Phys. B* **703** (2004) 127–146, [arXiv:hep-ph/0405040](#).
- [30] V. Cirigliano, A. Crivellin, W. Dekens, J. de Vries, M. Hoferichter, and E. Mereghetti, “CP Violation in Higgs-Gauge Interactions: From Tabletop Experiments to the LHC,” *Phys. Rev. Lett.* **123** no. 5, (2019) 051801, [arXiv:1903.03625 \[hep-ph\]](#).
- [31] O. Lebedev and M. Pospelov, “Electric dipole moments in the limit of heavy superpartners,” *Phys. Rev. Lett.* **89** (2002) 101801, [arXiv:hep-ph/0204359](#).
- [32] M. Pospelov and A. Ritz, “Electric dipole moments as probes of new physics,” *Annals Phys.* **318** (2005) 119–169, [arXiv:hep-ph/0504231](#).
- [33] J. R. Ellis, J. S. Lee, and A. Pilaftsis, “Electric Dipole Moments in the MSSM Reloaded,” *JHEP* **10** (2008) 049, [arXiv:0808.1819 \[hep-ph\]](#).
- [34] M. Pospelov and A. Ritz, “Hadron electric dipole moments from CP odd operators of dimension five via QCD sum rules: The Vector meson,” *Phys. Lett. B* **471** (2000) 388–395, [arXiv:hep-ph/9910273](#).
- [35] V. M. Belyaev and B. L. Ioffe, “Determination of Baryon and Baryonic Resonance Masses from QCD Sum Rules. 1. Nonstrange Baryons,” *Sov. Phys. JETP* **56** (1982) 493–501.
- [36] J. E. Kim and K.-M. Lee, “The Scale Problem in Wormhole Physics,” *Phys. Rev. Lett.* **63** (1989) 20.
- [37] S.-J. Rey, “The Axion Dynamics in Wormhole Background,” *Phys. Rev. D* **39** (1989) 3185.
- [38] S. M. Barr and D. Seckel, “Planck scale corrections to axion models,” *Phys. Rev. D* **46** (1992) 539–549.

- [39] M. Kamionkowski and J. March-Russell, “Planck scale physics and the Peccei-Quinn mechanism,” *Phys. Lett. B* **282** (1992) 137–141, [arXiv:hep-th/9202003](#).
- [40] R. Holman, S. D. H. Hsu, T. W. Kephart, E. W. Kolb, R. Watkins, and L. M. Widrow, “Solutions to the strong CP problem in a world with gravity,” *Phys. Lett. B* **282** (1992) 132–136, [arXiv:hep-ph/9203206](#).
- [41] S. Ghigna, M. Lusignoli, and M. Roncadelli, “Instability of the invisible axion,” *Phys. Lett. B* **283** (1992) 278–281.
- [42] R. Kallosh, A. D. Linde, D. A. Linde, and L. Susskind, “Gravity and global symmetries,” *Phys. Rev. D* **52** (1995) 912–935, [arXiv:hep-th/9502069](#).
- [43] R. Blumenhagen, M. Cvetič, S. Kachru, and T. Weigand, “D-Brane Instantons in Type II Orientifolds,” *Ann. Rev. Nucl. Part. Sci.* **59** (2009) 269–296, [arXiv:0902.3251 \[hep-th\]](#).
- [44] A. Hebecker, T. Mikhail, and P. Soler, “Euclidean wormholes, baby universes, and their impact on particle physics and cosmology,” *Front. Astron. Space Sci.* **5** (2018) 35, [arXiv:1807.00824 \[hep-th\]](#).
- [45] E. Braaten, C.-S. Li, and T.-C. Yuan, “The Evolution of Weinberg’s Gluonic CP Violation Operator,” *Phys. Rev. Lett.* **64** (1990) 1709.
- [46] G. Degrandi, E. Franco, S. Marchetti, and L. Silvestrini, “QCD corrections to the electric dipole moment of the neutron in the MSSM,” *JHEP* **11** (2005) 044, [arXiv:hep-ph/0510137](#).
- [47] J. Hisano, K. Tsumura, and M. J. S. Yang, “QCD Corrections to Neutron Electric Dipole Moment from Dimension-six Four-Quark Operators,” *Phys. Lett. B* **713** (2012) 473–480, [arXiv:1205.2212 \[hep-ph\]](#).
- [48] M. Pospelov and A. Ritz, “Theta induced electric dipole moment of the neutron via QCD sum rules,” *Phys. Rev. Lett.* **83** (1999) 2526–2529, [arXiv:hep-ph/9904483](#).
- [49] M. Pospelov and A. Ritz, “Neutron EDM from electric and chromoelectric dipole moments of quarks,” *Phys. Rev. D* **63** (2001) 073015, [arXiv:hep-ph/0010037](#).
- [50] D. A. Demir, M. Pospelov, and A. Ritz, “Hadronic EDMs, the Weinberg operator, and light gluinos,” *Phys. Rev. D* **67** (2003) 015007, [arXiv:hep-ph/0208257](#).
- [51] J. Hisano, J. Y. Lee, N. Nagata, and Y. Shimizu, “Reevaluation of Neutron Electric Dipole Moment with QCD Sum Rules,” *Phys. Rev. D* **85** (2012) 114044, [arXiv:1204.2653 \[hep-ph\]](#).
- [52] J. Hisano, D. Kobayashi, W. Kuramoto, and T. Kuwahara, “Nucleon Electric Dipole Moments in High-Scale Supersymmetric Models,” *JHEP* **11** (2015) 085, [arXiv:1507.05836 \[hep-ph\]](#).
- [53] U. Haisch and A. Hala, “Sum rules for CP-violating operators of Weinberg type,” *JHEP* **11** (2019) 154, [arXiv:1909.08955 \[hep-ph\]](#).
- [54] N. Yamanaka and E. Hiyama, “Weinberg operator contribution to the nucleon electric dipole moment in the quark model,” *Phys. Rev. D* **103** no. 3, (2021) 035023, [arXiv:2011.02531 \[hep-ph\]](#).
- [55] K. Kaneta, N. Nagata, K. A. Olive, M. Pospelov, and L. Velasco-Sevilla, “Quantifying limits on CP violating phases from EDMs in supersymmetry,” *JHEP* **03** (2023) 250, [arXiv:2303.02822 \[hep-ph\]](#).

- [56] O. Cata, “Relations between vacuum condensates and low energy parameters from a rational approach,” *Phys. Rev. D* **81** (2010) 054011, [arXiv:0911.4736 \[hep-ph\]](#).
- [57] S. Park, R. Gupta, T. Bhattacharya, F. He, S. Mondal, H.-W. Lin, and B. Yoon, “Flavor diagonal nucleon charges using clover fermions on MILC HISQ ensembles,” *Phys. Rev. D* **112** no. 5, (2025) 054508, [arXiv:2503.07100 \[hep-lat\]](#).
- [58] C. Alexandrou, S. Bacchio, J. Finkenrath, C. Iona, G. Koutsou, Y. Li, and G. Spanoudes, “Nucleon charges and σ -terms in lattice QCD,” *Phys. Rev. D* **111** no. 5, (2025) 054505, [arXiv:2412.01535 \[hep-lat\]](#).
- [59] L. Vecchi, “A strange contribution to the neutron EDM,” *JHEP* **09** (2025) 064, [arXiv:2506.23402 \[hep-ph\]](#).
- [60] **Particle Data Group** Collaboration, S. Navas *et al.*, “Review of particle physics,” *Phys. Rev. D* **110** no. 3, (2024) 030001.
- [61] I. I. Y. Bigi and N. G. Uraltsev, “Effective gluon operators and the dipole moment of the neutron,” *Sov. Phys. JETP* **73** (1991) 198–210.
- [62] I. I. Y. Bigi and N. G. Uraltsev, “Induced Multi - Gluon Couplings and the Neutron Electric Dipole Moment,” *Nucl. Phys. B* **353** (1991) 321–336.
- [63] J. Bsaisou, J. de Vries, C. Hanhart, S. Liebig, U.-G. Meissner, D. Minossi, A. Nogga, and A. Wirzba, “Nuclear Electric Dipole Moments in Chiral Effective Field Theory,” *JHEP* **03** (2015) 104, [arXiv:1411.5804 \[hep-ph\]](#). [Erratum: *JHEP* 05, 083 (2015)].
- [64] J. de Vries, E. Mereghetti, and A. Walker-Loud, “Baryon mass splittings and strong CP violation in SU(3) Chiral Perturbation Theory,” *Phys. Rev. C* **92** no. 4, (2015) 045201, [arXiv:1506.06247 \[nucl-th\]](#).
- [65] T. R. Richardson, “Strong CP violation and large- N_c spin-flavor symmetry,” *Phys. Rev. D* **112** no. 9, (2025) 095045, [arXiv:2509.03613 \[hep-ph\]](#).
- [66] V. Baru, C. Hanhart, M. Hoferichter, B. Kubis, A. Nogga, and D. R. Phillips, “Precision calculation of threshold π^-d scattering, πN scattering lengths, and the GMO sum rule,” *Nucl. Phys. A* **872** (2011) 69–116, [arXiv:1107.5509 \[nucl-th\]](#).
- [67] V. Bernard, N. Kaiser, and U.-G. Meissner, “Aspects of chiral pion - nucleon physics,” *Nucl. Phys. A* **615** (1997) 483–500, [arXiv:hep-ph/9611253](#).
- [68] M. Pospelov, “Best values for the CP odd meson nucleon couplings from supersymmetry,” *Phys. Lett. B* **530** (2002) 123–128, [arXiv:hep-ph/0109044](#).
- [69] C.-Y. Seng, “Relating hadronic CP-violation to higher-twist distributions,” *Phys. Rev. Lett.* **122** no. 7, (2019) 072001, [arXiv:1809.00307 \[hep-ph\]](#).
- [70] S. Bhattacharya, K. Fuyuto, E. Mereghetti, and T. R. Richardson, “Toward the determination of CP-odd pion-nucleon couplings,” *Phys. Rev. C* **112** no. 2, (2025) 025501, [arXiv:2504.01105 \[hep-ph\]](#).
- [71] N. Osamura, P. Gubler, and N. Yamanaka, “Contribution of the Weinberg-type operator to atomic and nuclear electric dipole moments,” *JHEP* **06** (2022) 072, [arXiv:2203.06878 \[hep-ph\]](#).
- [72] S. Weinberg, “Larger Higgs Exchange Terms in the Neutron Electric Dipole Moment,” *Phys. Rev. Lett.* **63** (1989) 2333.

- [73] N. Yamanaka and M. Oka, “Weinberg operator contribution to the CP-odd nuclear force in the quark model,” *Phys. Rev. D* **106** no. 7, (2022) 075021, [arXiv:2208.03920 \[nucl-th\]](#).
- [74] E. Epelbaum, H.-W. Hammer, and U.-G. Meissner, “Modern Theory of Nuclear Forces,” *Rev. Mod. Phys.* **81** (2009) 1773–1825, [arXiv:0811.1338 \[nucl-th\]](#).
- [75] V. V. Flambaum, M. Pospelov, A. Ritz, and Y. V. Stadnik, “Sensitivity of EDM experiments in paramagnetic atoms and molecules to hadronic CP violation,” *Phys. Rev. D* **102** no. 3, (2020) 035001, [arXiv:1912.13129 \[hep-ph\]](#).
- [76] H. Mulder, R. Timmermans, and J. de Vries, “Probing the QCD $\bar{\theta}$ term with paramagnetic molecules,” *JHEP* **07** (2025) 232, [arXiv:2502.06406 \[hep-ph\]](#).
- [77] W. Dekens, J. de Vries, L. Gialidi, J. Menéndez, H. Mulder, and B. Romeo, “Nucleon Electric Dipole Moments in Paramagnetic Molecules through Effective Field Theory,” *Phys. Rev. Lett.* **136** no. 20, (2026) 201803, [arXiv:2510.14933 \[hep-ph\]](#).
- [78] **CPEDM** Collaboration, F. Abusaif *et al.*, *Storage ring to search for electric dipole moments of charged particles: Feasibility study*. CERN, Geneva, 6, 2021. [arXiv:1912.07881 \[hep-ex\]](#).
- [79] **JEDI** Collaboration, V. Shmakova, “Electric dipole moment of charged particles using storage rings,” *EPJ Web Conf.* **290** (2023) 07002.
- [80] A. Lehrach, B. Lorentz, W. Morse, N. Nikolaev, and F. Rathmann, “Precursor Experiments to Search for Permanent Electric Dipole Moments (EDMs) of Protons and Deuterons at COSY,” [arXiv:1201.5773 \[hep-ex\]](#).
- [81] M. Hubert and T. Fleig, “Electric dipole moments generated by nuclear Schiff moment interactions: A reassessment of the atoms Xe129 and Hg199 and the molecule TlF205,” *Phys. Rev. A* **106** no. 2, (2022) 022817, [arXiv:2203.04618 \[physics.atom-ph\]](#).
- [82] J. Engel, M. J. Ramsey-Musolf, and U. van Kolck, “Electric Dipole Moments of Nucleons, Nuclei, and Atoms: The Standard Model and Beyond,” *Prog. Part. Nucl. Phys.* **71** (2013) 21–74, [arXiv:1303.2371 \[nucl-th\]](#).
- [83] V. F. Dmitriev, R. A. Sen’kov, and N. Auerbach, “Effects of core polarization on the nuclear Schiff moment,” *Phys. Rev. C* **71** (2005) 035501, [arXiv:nucl-th/0408065](#).
- [84] V. A. Dzuba, V. V. Flambaum, and S. G. Porsev, “Calculation of P,T-odd electric dipole moments for diamagnetic atoms Xe-129, Yb-171, Hg-199, Rn-211, and Ra-225,” *Phys. Rev. A* **80** (2009) 032120, [arXiv:0906.5437 \[physics.atom-ph\]](#).
- [85] V. V. Flambaum and V. A. Dzuba, “Electric dipole moments of atoms and molecules produced by enhanced nuclear Schiff moments,” *Phys. Rev. A* **101** no. 4, (2020) 042504, [arXiv:1912.03598 \[physics.atom-ph\]](#).
- [86] V. A. Dzuba, V. V. Flambaum, and J. S. M. Ginges, “Atomic electric dipole moments of He and Yb induced by nuclear Schiff moments,” *Phys. Rev. A* **76** (2007) 034501, [arXiv:0705.4001 \[physics.atom-ph\]](#).
- [87] J. Dobaczewski, J. Engel, M. Kortelainen, and P. Becker, “Correlating Schiff moments in the light actinides with octupole moments,” *Phys. Rev. Lett.* **121** no. 23, (2018) 232501, [arXiv:1807.09581 \[nucl-th\]](#).
- [88] L. I. Schiff, “Measurability of Nuclear Electric Dipole Moments,” *Phys. Rev.* **132** (1963) 2194–2200.

- [89] J. Engel, “Nuclear Schiff Moments and CP Violation,” *Ann. Rev. Nucl. Part. Sci.* **75** no. 1, (2025) 129–151, [arXiv:2501.02744 \[nucl-th\]](#).
- [90] N. Auerbach, V. V. Flambaum, and V. Spevak, “Collective T and P odd electromagnetic moments in nuclei with octupole deformations,” *Phys. Rev. Lett.* **76** (1996) 4316–4319, [arXiv:nucl-th/9601046](#).
- [91] V. Spevak, N. Auerbach, and V. V. Flambaum, “Enhanced T odd P odd electromagnetic moments in reflection asymmetric nuclei,” *Phys. Rev. C* **56** (1997) 1357–1369, [arXiv:nucl-th/9612044](#).
- [92] V. V. Flambaum and A. J. Mansour, “Enhanced nuclear Schiff and electric dipole moments in nuclei with octupole deformation,” *Phys. Rev. C* **111** no. 5, (2025) 055501, [arXiv:2411.18943 \[nucl-th\]](#).
- [93] M. Bishof *et al.*, “Improved limit on the ^{225}Ra electric dipole moment,” *Phys. Rev. C* **94** no. 2, (2016) 025501, [arXiv:1606.04931 \[nucl-ex\]](#).
- [94] B. Graner, Y. Chen, E. G. Lindahl, and B. R. Heckel, “Reduced Limit on the Permanent Electric Dipole Moment of $\text{Hg}199$,” *Phys. Rev. Lett.* **116** no. 16, (2016) 161601, [arXiv:1601.04339 \[physics.atom-ph\]](#). [Erratum: *Phys.Rev.Lett.* 119, 119901 (2017)].
- [95] C. Abel *et al.*, “Measurement of the Permanent Electric Dipole Moment of the Neutron,” *Phys. Rev. Lett.* **124** no. 8, (2020) 081803, [arXiv:2001.11966 \[hep-ex\]](#).
- [96] N. Sachdeva *et al.*, “New Limit on the Permanent Electric Dipole Moment of ^{129}Xe using ^3He Comagnetometry and SQUID Detection,” *Phys. Rev. Lett.* **123** no. 14, (2019) 143003, [arXiv:1902.02864 \[physics.atom-ph\]](#).
- [97] F. Allmendinger, I. Engin, W. Heil, S. Karpuk, H. J. Krause, B. Niederländer, A. Offenhäusser, M. Repetto, U. Schmidt, and S. Zimmer, “Measurement of the Permanent Electric Dipole Moment of the ^{129}Xe Atom,” *Phys. Rev. A* **100** no. 2, (2019) 022505, [arXiv:1904.12295 \[physics.atom-ph\]](#).
- [98] T. A. Zheng, Y. A. Yang, S. Z. Wang, J. T. Singh, Z. X. Xiong, T. Xia, and Z. T. Lu, “Measurement of the Electric Dipole Moment of $\text{Yb}171$ Atoms in an Optical Dipole Trap,” *Phys. Rev. Lett.* **129** no. 8, (2022) 083001, [arXiv:2207.08140 \[physics.atom-ph\]](#).
- [99] T. S. Roussy *et al.*, “An improved bound on the electron’s electric dipole moment,” *Science* **381** no. 6653, (2023) adg4084, [arXiv:2212.11841 \[physics.atom-ph\]](#).
- [100] **ACME** Collaboration, V. Andreev *et al.*, “Improved limit on the electric dipole moment of the electron,” *Nature* **562** no. 7727, (2018) 355–360.
- [101] J. J. Hudson, D. M. Kara, I. J. Smallman, B. E. Sauer, M. R. Tarbutt, and E. A. Hinds, “Improved measurement of the shape of the electron,” *Nature* **473** (2011) 493–496.
- [102] C. Baruch, P. B. Changala, Y. Shagam, and Y. Soreq, “Constraining CP Violating Nucleon-Nucleon Long-Range Interactions in Diatomic eEDM Searches,” *Phys. Rev. Lett.* **133** no. 11, (2024) 113202, [arXiv:2402.07504 \[hep-ph\]](#).
- [103] A. N. Petrov, N. S. Mosyagin, T. A. Isaev, and A. V. Titov, “Theoretical study of Hf F^+ in search of the electron electric dipole moment,” *Phys. Rev. A* **76** (2007) 030501, [arXiv:physics/0611254](#).
- [104] L. V. Skripnikov, “Communication: Theoretical study of HfF^+ cation to search for the T,P-odd interactions,” *J. Chem. Phys.* **147** no. 2, (2017) 021101.

- [105] T. Fleig, “ \mathcal{P} , \mathcal{T} -odd and magnetic hyperfine-interaction constants and excited-state lifetime for HfF^+ ,” *Phys. Rev. A* **96** no. 4, (2017) 040502, [arXiv:1706.02893](#) [[physics.atom-ph](#)].
- [106] E. R. Meyer and J. L. Bohn, “Prospects for an electron electric dipole moment search in metastable ThO and ThF,” *Phys. Rev. A* **78** (2008) 010502, [arXiv:0805.0161](#) [[physics.atom-ph](#)].
- [107] V. A. Dzuba, V. V. Flambaum, and C. Harabati, “Relations between matrix elements of different weak interactions and interpretation of the parity-nonconserving and electron electric-dipole-moment measurements in atoms and molecules,” *Phys. Rev. A* **84** no. 5, (2011) 052108.
- [108] L. V. Skripnikov, “Combined 4-component and relativistic pseudopotential study of tho for the electron electric dipole moment search,” *The Journal of Chemical Physics* **145** no. 21, (12, 2016) 214301. <https://doi.org/10.1063/1.4968229>.
- [109] M. Denis and T. Fleig, “In search of discrete symmetry violations beyond the standard model: Thorium monoxide reloaded,” *J. Chem. Phys.* **145** no. 21, (2016) 214307.
- [110] M. Abe, G. Gopakumar, M. Hada, B. P. Das, H. Tatewaki, and D. Mukherjee, “Application of relativistic coupled-cluster theory to the effective electric field in YbF,” *Phys. Rev. A* **90** no. 2, (2014) 022501.
- [111] A. Sunaga, M. Abe, M. Hada, and B. P. Das, “Relativistic coupled-cluster calculation of the electron-nucleus scalar-pseudoscalar interaction constant W_s in ybf,” *Phys. Rev. A* **93** (Apr, 2016) 042507. <https://link.aps.org/doi/10.1103/PhysRevA.93.042507>.
- [112] J. J. Hudson, B. E. Sauer, M. R. Tarbutt, and E. A. Hinds, “Measurement of the electron electric dipole moment using YbF molecules,” *Phys. Rev. Lett.* **89** (2002) 023003, [arXiv:hep-ex/0202014](#).
- [113] J. S. M. Ginges and V. V. Flambaum, “Violations of fundamental symmetries in atoms and tests of unification theories of elementary particles,” *Phys. Rept.* **397** (2004) 63–154, [arXiv:physics/0309054](#).
- [114] A. Manohar and H. Georgi, “Chiral Quarks and the Nonrelativistic Quark Model,” *Nucl. Phys. B* **234** (1984) 189–212.
- [115] H. Georgi and L. Randall, “Flavor Conserving CP Violation in Invisible Axion Models,” *Nucl. Phys. B* **276** (1986) 241–252.